

Surface modes of ultra-cold atomic clouds with very large number of vortices

M. A. Cazalilla

*The Abdus Salam ICTP, Strada Costiera 11, 34014 Trieste, Italy, and
Donostia International Physics Center (DIPC), Manuel de Lardizabal 4, 20018 Donostia, Spain.*

We study the surface modes of some of the vortex liquids recently found by means of exact diagonalizations in systems of rapidly rotating bosons. In contrast to the surface modes of Bose condensates, we find that the surface waves have a frequency linear in the excitation angular momentum, $\hbar l > 0$. Furthermore, in analogy with the edge waves of electronic quantum Hall states, these excitations are *chiral*, that is, they can be excited only for values of l that increase the total angular momentum of the vortex liquid. However, differently from the quantum Hall phenomena for electrons, we also find other excitations that are approximately degenerate in the laboratory frame with the surface modes, and which decrease the total angular momentum by l quanta. The surface modes of the Laughlin, as well as other scalar and vector boson states are analyzed, and their *observable* properties characterized. We argue that measurement of the response of a vortex liquid to a weak time-dependent potential that imparts angular momentum to the system should provide valuable information to characterize the vortex liquid. In particular, the intensity of the signal of the surface waves in the dynamic structure factor has been studied and found to depend on the type of vortex liquid. We point out that the existence of surface modes has observable consequences on the density profile of the Laughlin state. These features are due to the strongly correlated behavior of atoms in the vortex liquids. We point out that these correlations should be responsible for a remarkable stability of some vortex liquids with respect to three-body losses.

PACS numbers: 3.75.Fi, 05.30.Jp, 73.43.-f

I. INTRODUCTION

Everybody is familiar with the phenomenon of vortices. We observe it every time we watch water down a drain. In classical fluids, it is a consequence of broken Galilean symmetry [1]: A fluid that fills a region of space provides us with a privileged reference frame, namely the one where the fluid is at rest. Nature tries to restore the full Galilean invariance at the vortex core, which explains why the fluid density drops to zero (or almost zero) there. In superfluids, however, vortices exhibit certain peculiarities not seen in classical fluids. This is because quantum coherence is maintained throughout the superfluid volume, and since the wave function must be singly valued the circulation around a vortex is quantized. Therefore, the stability of vortices is ensured by *topological* rather than *dynamical* reasons [2]. Nevertheless, a vortex carrying $n > 1$ circulation quanta is unstable with respect to decay into n singly quantized vortices. When many of these have appeared, they form a triangular lattice, the Abrikosov lattice. In ultra-cold atomic gases the formation of this lattice has been observed in a recent experiment [3]. If the rotation frequency, Ω , is further increased to approach the trap frequency [4], ω_\perp , several authors [5, 7, 8] have pointed to the interesting possibility that the Abrikosov lattice melts due to quantum fluctuations. This regime ($\Omega \lesssim \omega_\perp$) is known as the *critical rotation* limit, and some experiments have already begun to explore it [9].

What kind of phenomena can be expected to emerge in the critical rotation limit? Under certain conditions, which will be discussed below, it has been predicted that bosons organize themselves in highly correlated, two-dimensional, “vortex liquids”. These are states that cannot be described by the standard (i.e. Gross-Pitaevskii) mean field theory [5, 10]. Instead, they seem to be quite accurately described by microscopic wave functions [5, 10], closely related to those used for electrons in the context of the fractional quantum Hall effect (FQHE) [14, 15]. Recent numerical studies using periodic boundary conditions [5] have shown that, just like their FQHE counterparts, homogeneous vortex liquids are incompressible. This means that changing their density requires a finite amount of energy, signaling the existence of a spectral gap. When carried out for small systems in a harmonic trap, exact diagonalization studies [10, 11] found a series particularly stable states at “magic values” of the angular momentum, some of them related to the homogeneous vortex liquids [6].

In this work we address the following question: Which are the experimental signatures of these vortex liquids? The question is relevant since experiments driving ultra-cold atom clouds to the critical rotation limit are likely to proliferate in the near future. It is also important to find ways to characterize the vortex liquids by *non-destructive* means, especially if one intends to use their entanglement properties for quantum computing purposes [16]. Below we shall try to answer the previous question by studying the properties of surface excitations of some of these states. Since the vortex liquids are effectively two dimensional, by “surface” we mean the *one-dimensional boundary* in the plane perpendicular to the rotation axis. Excitations along the rotation axis will occur at much higher energies and are therefore frozen at the low temperatures of interest here. As we shall argue in section III, deformations of the

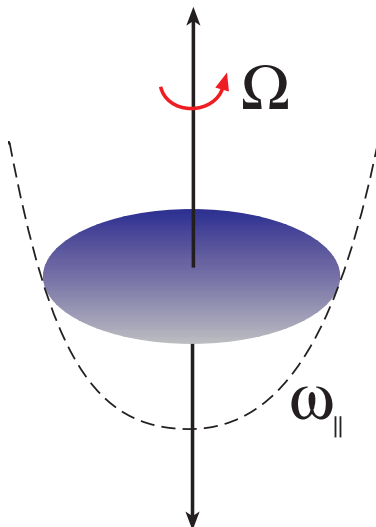


FIG. 1: Rapidly rotating cloud of ultra-cold atoms in the critical rotation regime $\Omega \lesssim \omega_{\perp}$.

boundary correspond to the lowest energy excitations of the system. Their spectroscopic analysis should provide valuable information on what kind of vortex liquid one is dealing with. In the case of the FQHE exhibited by two-dimensional electron gases under strong magnetic fields, characterization of the state of the sample is usually achieved by means of transport measurements. In particular, a measurement of the Hall conductance automatically yields the filling fraction ν , which in the present context and in the limit of large particle and vortex numbers can be defined as the ratio of the number of particles to the number of vortices, i.e. $\nu = N/N_v$. However, nothing like transport spectroscopy is yet available for ultra-cold atomic clouds. Instead, experiments where the trapping potential is weakly deformed in a time-dependent fashion, therefore exciting surface modes, seem more feasible. That this is feasible with a *rotating* cloud containing a large number of vortices has been already demonstrated in a recent experiment [12] (however, not yet in the regime in which we are interested here).

The study of the surface modes is also interesting because, at low temperatures, these excitations should dominate the properties of the system that can be probed by weakly coupling to it. Furthermore, it has been shown in the context of the FQHE [19, 20] that analyzing the boundary excitations is the way to characterize the bulk states (i.e. their *quantum orders* [20]). What is more, the boundary of a vortex liquid is also a clean example of an exotic type of quantum liquid: The *chiral* Luttinger liquid. The main difference with the *electronic* FQHE is that the constituent particles of the system are *neutral* bosonic atoms, which interact via short-range interactions. This setup offers some advantages over the two-dimensional electron gas at high magnetic field. The systems are intrinsically clean, and the absence of long-range interactions does not lead to some complications introduced by the Coulomb potential (e.g. edge reconstructions [15]). One can also consider atoms with internal degrees of freedom, which opens the possibility to study novel quantum Hall states [18, 23]. The disadvantages are the fragility of the vortex liquids, which will require careful experiments with small numbers of particles, $N \lesssim 100$ (although many replicas of a rotating cloud can be created in an optical lattice [21]). In the future, other methods to “simulate” high magnetic fields using optical lattices may become available [22], and this could lift the constraint on the particle number. However, large systems confined by smooth potentials, like the ones used to trap ultra-cold atoms, should exhibit more complicated boundary structures like “composite edges” [19], with many branches of surface modes. Nevertheless, the theory developed here should provide the basis for the understanding of such systems.

The experimental achievement of the vortex liquid states to be discussed below is challenging, but on the theoretical side a complete understanding of their properties also poses many challenges. The existing work has mainly focused on ground states of scalar [5, 10] and higher-spin bosons [17, 21, 23], but the situation is far from being as clear as in the FQHE for electrons [15]. In this paper, we shall consider the surface excitations of several ground states of scalar and vector bosons. One of them, the Laughlin state, is an exact ground state for rotating scalar bosons. The other ground states for scalar bosons that we will consider are approximate, and have been found to exhibit good overlap with the exact ground states obtained by exact diagonalization methods [5, 6, 10, 11]. We shall consider the Laughlin state first, for which the microscopic construction of the surface waves will be presented. An effective field theory will be subsequently developed and shown to agree with the microscopic theory. Although the assumptions for the effective theory strictly hold in the large N limit, it is well established numerically (e.g. [19, 33, 34]) that it also applies to small systems with $N \sim 10$, within the experimental reach in the near future.

As many of the concepts and methods introduced and used in this paper should be new to the community working in ultra-cold atom systems, we have adopted a pedagogical approach at the cost of producing a longer paper. We have also tried to make the article as self-contained as possible, but without omitting references to the original literature on the quantum Hall effect, which should be consulted for more extended explanations. The paper is organized as follows: In the next section, the experimental conditions for the existence of vortex liquids are discussed. Next, the simplest (from the theoretical point of view) type of vortex liquid, namely the Laughlin liquid, is considered. In section IV surface excitations of more complicated (but approximate) states of scalar bosons are studied. In the following section, we take up vector bosons and analyze the surface excitations of their singlet states. Finally, the conclusions of this work can be found in Sect. VI. In the appendices we include some supplementary material. Thus appendix A discusses the relation between the laboratory and rotating frames, and how measurements in the laboratory frame are related to calculations in the rotating frame. We also discuss the generalized Kohn's theorem in this appendix, and how it constrains the energy and peak intensity of the dipole mode. Appendix B, however, gives a brief introduction to the plasma formalism for quantum Hall wave functions. More importantly, we also show there how to obtain the wave functions from correlation functions of the field theory that describes the boundary excitations.

II. EXPERIMENTAL CONDITIONS FOR THE OBSERVATION OF VORTEX LIQUIDS

Before proceeding any further, it will be useful to recall the conditions under which it is expected that a rotating cloud of ultra-cold atoms will become a vortex liquid. The strong analogy between the quantum mechanics of rotating particles in a harmonic well and charged particles moving in two-dimensions under a strong magnetic field will be useful here; therefore, the appearance of Landau levels is expected. To see this, notice that the one-body part of the Hamiltonian in the *rotating* reference frame (see Appendix A),

$$H_j = \frac{\mathbf{p}_j^2 + p_{zj}^2}{2M} + \frac{M}{2} \left(\omega_\perp^2 \mathbf{r}_j^2 + \omega_\parallel^2 z_j^2 \right) - \Omega \hat{\mathbf{z}} \cdot \mathbf{L}_j \quad (1)$$

can be written in two equivalent ways:

$$H_j^{(1)} = \frac{(\mathbf{p}_j - M\Omega \hat{\mathbf{z}} \times \mathbf{r}_j)^2}{2M} + \frac{M}{2} (\omega_\perp^2 - \Omega^2) \mathbf{r}_j^2 + \frac{p_{zj}^2}{2M} + \frac{M\omega_\parallel^2}{2} z_j^2, \quad (2)$$

and

$$H_j^{(2)} = \frac{(\mathbf{p}_j - M\omega_\perp \hat{\mathbf{z}} \times \mathbf{r}_j)^2}{2M} + (\omega_\perp - \Omega) \hat{\mathbf{z}} \cdot \mathbf{L}_j + \frac{p_{zj}^2}{2M} + \frac{M\omega_\parallel^2}{2} z_j^2. \quad (3)$$

We have assumed an axially symmetric trap with the rotation axis coinciding with the symmetry axis of the trap; the following notation has been introduced: $\mathbf{r}_j = (x_j, y_j)$ and $\mathbf{p}_j = (p_{xj}, p_{yj})$ are the j -th particle position and momentum, respectively, while $\mathbf{L}_j = \mathbf{r}_j \times \mathbf{p}_j$ is the angular momentum along the rotation axis. In both forms of H_j , it is manifest that particles, in the rotating reference frame, feel an *effective* magnetic field directed along $\hat{\mathbf{z}}$, whose magnitude is proportional to either $M\Omega$ or $M\omega_\perp$, depending on the form, M being the atom mass. Perhaps the first form, $H_j^{(1)}$, shows more explicitly what happens as Ω approaches ω_\perp , and the system enters the critical rotation regime: First, notice that particles under rotation experience a reduced confinement in the plane perpendicular to the rotation axis. This means that, as Ω is increased towards the trap frequency ω_\perp , more and more particles will accommodate into the lowest axial level (this can be helped by making $\omega_\parallel > \omega_\perp$ [4]). Eventually, when all the particles are in this level, the system effectively becomes two-dimensional. At the same time, increasing Ω increases the strength of the effective magnetic field and therefore, for sufficiently weak interactions, all particles will make its way into the lowest Landau level (LLL).

To study the quasi two-dimensional system in the critical rotation regime with all the particles lying in the lowest Landau and axial levels, it is more convenient to use the second form of the Hamiltonian, $H_j^{(2)}$. Dropping the axial part and introducing the following operators:

$$\pi_j = \pi_{jx} + i\pi_{jy}, \quad (4)$$

$$\bar{\pi}_j = \pi_{jx} - i\pi_{jy}, \quad (5)$$

where $\pi_{jx} = p_{jx} + M\omega_\perp y_j$ and $\pi_{jy} = p_{jy} - M\omega_\perp x_j$, and $[\pi_j, \bar{\pi}_j] = 4M\hbar\omega_\perp$, allows us to write:

$$H_j^{(2)} = \frac{\bar{\pi}_j \pi_j}{2M} + (\omega_\perp - \Omega) L_j + \hbar\omega_\perp. \quad (6)$$

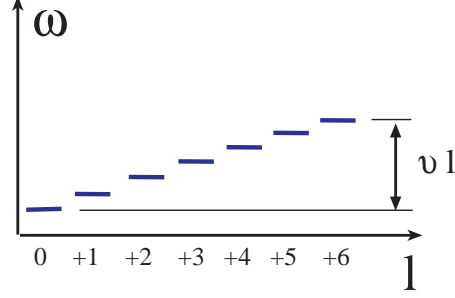


FIG. 2: For non-interacting particles, the large degeneracy of the lowest Landau level is lifted only by the confining potential. In the reference frame that rotates with the system, a “band” of width $\approx \hbar v N / \nu$ is formed.

One can easily convince oneself that this form is diagonal after noticing that π_j and $\bar{\pi}_j$ are nothing but ladder operators, which move particles between consecutive Landau levels: $\bar{\pi}_j$ promotes the j -th particle to a higher Landau level whereas π_j undoes this operation. Thus, if a particle is in the LLL, the corresponding π_j must annihilate the state. Once diagonalized, one finds that the single-particle orbitals in the LLL have energies (in the rotating frame) equal to $\epsilon(l) = \hbar\omega_\perp + \hbar v l$, where $v \equiv (\omega_\perp - \Omega) \ll \omega_\perp$ and $\hbar l$ is the angular momentum. They form a “band” (see Fig. 2) within the LLL. The orbitals themselves take the form:

$$\varphi_l(x, y) = \frac{1}{\ell \sqrt{\pi l!}} \left(\frac{z}{\ell} \right)^l e^{-|z|^2/2\ell^2}, \quad (7)$$

where $\ell = \sqrt{\hbar/M\omega_\perp}$ is the oscillator length of the trap, and $z = x + iy$ denotes the position of the particle on the plane perpendicular to the rotation axis. As the system is effectively two dimensional, we have omitted the orbital describing the motion perpendicular to the plane.

We are now ready to take up the discussion of the conditions under which the scenario described above can be experimentally realized. Interactions between the particles are needed for the stability of the vortex liquids to be discussed below. Taking them into account, the total Hamiltonian reads $H = \sum_{j=1}^N H_j + \sum_{i<j=1}^N V_{ij}$, $V_{ij} = g \delta^{(2)}(\mathbf{r}_i - \mathbf{r}_j) \delta(z_i - z_j)$, where g is related to the s-wave scattering length, a , as usual: $g = 4\pi\hbar^2 a/M$. The interactions should be neither too weak nor too strong. Since $\hbar v$ is the level spacing of the single-particle band in the LLL, we must have that $gn \gg \hbar v$ but $gn < N\hbar v/\nu$, where n is the mean density of the system. The last condition is the requirement that the width of single-particle band must be larger than typical interaction energy, gn . The filling of the band is determined by the total angular momentum through the *filling fraction* $\nu \approx N^2/2L$. Hence $N/\nu \approx 2L/N$ measures the mean angular momentum per particle. Finally, since all the particles must be in the LLL, mixing with higher Landau levels is avoided provided that $N\hbar v/\nu \ll \hbar\Omega$ and $gn \ll \hbar\Omega$ and at temperatures $T \ll \hbar\Omega$. Although these conditions look very demanding, we expect the rapid progress that has characterized the field over the last years will make vortex liquids experimentally available in a near future.

III. SURFACE MODES OF THE BOSONIC LAUGHLIN STATE

We begin by considering the simplest case, from the theoretical point of view. A droplet of N bosons in the Laughlin state is described by the following wave function

$$\Phi_m(z_1, \dots, z_N) = \prod_{i<j=1}^N (z_i - z_j)^m, \quad (8)$$

where $m = 2$ (m must be even for bosons and odd for fermions). In this expression we have only written the *polynomial* part of the wave function. We have omitted (and will omit henceforth) a factor that includes the normalization constant and a product of single-particle orbitals involving the gaussians that depend on $|z_i|^2$ and the orbital that describes the state along the rotation axis. By demanding all particles to be in the LLL, the above function can only depend on z_j , and not on its complex conjugate, $\bar{z}_j = x_j - iy_j$. To understand this physically, notice that in the LLL the kinetic energy is minimized while the angular momentum is maximized. Therefore, the angular momentum of every particle along the rotation axis must be positive or zero. This is true as long as the polynomial part of

the wave function depends *only* on $z_j^l \propto e^{il\theta_j}$, with $l \geq 0$. In other words, the polynomial part of the wave function must be an *analytic* function of z_j , for $j = 1, \dots, N$. Therefore, allowing $\sum_{j=1}^N H_j$ to act on Φ_m yields N times the energy of a particle in the lowest Landau and axial levels, $\hbar(\omega_\perp + \omega_\parallel/2)$, plus the confinement energy, vL_o , where $L_o = \hbar m N(N-1)/2 = \hbar N(N-1)$ is the total angular momentum of the Laughlin state (to see this, consider a rigid rotation of the system where $z_i \rightarrow z_i e^{i\theta}$, the angular momentum can be read off the phase factor of the many-body wave function). Furthermore, one can easily see that the Jastrow structure of (8) produces a state with zero interaction energy for $V_{ij} = g_{2d} \delta^{(2)}(\mathbf{r}_i - \mathbf{r}_j)$, which in this case represents the relevant interaction for ultra-cold atoms confined to two dimensions [40].

Let us now consider the excitations about the Laughlin state. Bulk excitations [14] come in two types: quasi-holes and quasi-particles. They correspond to a deficit (quasi-holes) or an excess (quasi-particles) of $\frac{1}{m} = \frac{1}{2}$ boson in the bulk of the droplet. Another interesting property, which will be useful in the following section, is that creating a quasi-hole increases the *average* angular momentum of the system, whereas creating a quasi-particle decreases it. For example, by creating a quasi-hole at the center of the a droplet: $\prod_{i=1}^N z_i \Phi_m$, so that the resulting state is an eigenstate of L , the angular momentum increases by $\hbar N$, and the energy (in the rotating frame) by $\hbar v N$. However, if we consider wave functions of the form [24, 26] $s_l \Phi_m$, where the factor is a symmetric polynomial, $s_l = \sum_{i=1}^N z_i^l$, with $0 \leq l \ll N$, the angular momentum increases only by $\hbar l$ and the energy by $\hbar v l$, much less than the quasi-hole energy. Thus we see that the states created by multiplying the Laughlin state by (products of) s_l are indeed the low-lying excitations of the system. These states describe deformations of the droplet boundary, which in the ground state has a circular shape. This is true for all $l > 1$ except for $l = 1$, as $s_1 = \sum_{i=1}^N z_i$ represents a small translation of the droplet center of mass, which leaves the shape of the boundary unchanged.

On the other hand, quasi-particles are not the only kind of excitations that decrease the angular momentum of the system. Consider the states created by the action of the operators $d_l = \sum_{j=1}^N \bar{\pi}_j^l$ ($l = 1, 2, \dots$) on the Laughlin state, where $\bar{\pi}_j$ has been defined in Eq. (5). According to the discussion that we made in previous section, it is easy to understand what these operators do: They move up one particle by l Landau levels. At the same time, one can show that they *decrease* the total angular momenta by l quanta. The one-body part of the Hamiltonian thus yields an excitation energy (in the rotating frame) equal to $\hbar(\omega_\perp + \Omega)l$, but strictly speaking the states are not exact eigenstates of the full many-body Hamiltonian since they do not diagonalize the interaction potential. However, their interaction energy for $l \ll N$ is much smaller than their one-body energy since $gn \ll \hbar\Omega$, and therefore they can be considered as good approximations to the exact eigenstates. Furthermore, one can show that for $l = 1$, $d_1 \sim \sum_{j=1}^N \bar{z}_j = \bar{s}_1$, which has zero interaction energy. Thus d_1 and s_1 are the two independent modes that describe the center-of-mass motion in the plane perpendicular to the rotation axis. They are sometimes known as “Kohn modes”, and their properties are discussed in detail in appendix A. Returning to the general properties of the states created by d_l , and applying the relation $E_{ROT} = E_{LAB} - \Omega L$ (see appendix A), we find that the energy of these states in the laboratory frame is $\approx \hbar\omega_\perp l$, which means that they are practically degenerate (in the laboratory frame) with the surface modes described by s_l . This forces us to clarify what we meant above by “low-lying” excitations of the system. First of all, it is necessary to recall that the system is at thermal equilibrium in the rotating frame and *not* in the laboratory frame. The characterization of excited states as low-lying or otherwise high-energy states must be done in this frame, where the states $d_l \Phi_m$ have much higher energy than the states $s_l \Phi_m$. Therefore, at the temperatures $T \ll \hbar\Omega$ of interest here, the statistical probability of finding the system in the latter states is much higher than in the former, and therefore the low-temperature properties are dominated by the states generated by s_l . Nevertheless, this does not mean that if the system is probed by an external field of frequency $\omega \approx \omega_\perp l$ ($l = 1, 2, \dots$) which excites modes of either chirality with equal probability, these excitations are not important to understand the response of the vortex liquid. As the frequency of the external field is determined by an apparatus located in the laboratory frame, modes of both chiralities will be excited. This is a distinct feature of vortex liquids compared to the physics exhibited by electronic quantum Hall systems. However, as it will be shown below, the response to an external probe is weighted by a thermal factor $[1 - \exp(-\hbar\omega_{ROT}(l)/T)]^{-1}$, and at temperatures such that $\hbar\Omega \gg T \gg \hbar v$, which should be more easily accessible, it yields a much higher intensity for the surface modes s_l than for the d_l modes. Actually, the considerations just made regarding the d_l modes also apply to more general (vortex-liquid) states than the Laughlin state. With these remarks, we close the discussion of the excitations generated by the operators d_l , and we shall not discuss them any further in this work. Instead, we shall focus on the surface modes generated by s_l , which exist only when the total angular momentum is increased by a small number of quanta $l \geq 0$, and for which all particles remain in the LLL.

In order to compute the low-temperature properties of a droplet of vortex liquid, it is convenient to develop an effective field theory that describes the low-energy part of the spectrum. The states generated by the action of s_l on Φ_m have a number of important properties which must be captured by the effective theory. First of all, they are all *chiral* since $l \geq 0$ and cannot be negative for otherwise the resulting state would not be in the LLL. Second, the linear dependence on l of the energy implies that the spectral degeneracy is given by $p(l)$, the number of partitions of l . This

is the number of distinct ways l can be written as a sum of non-negative integers. To understand this, recall that the angular momentum, and hence the energy, are proportional to the degree of the homogeneity of the polynomial part of the wave function. Therefore, given that $s_l \Phi_m$ has an excitation energy equal to $\hbar \nu l$, so do the states $s_{l-1} s_1 \Phi_m$ ($l = (l-1) + 1$), or $s_{l-2} (s_1)^2 \Phi_m$ ($l = (l-2) + 1 + 1$), etc. In the following, we will show that these features are in fact captured by quantizing a two-dimensional liquid drop model [19].

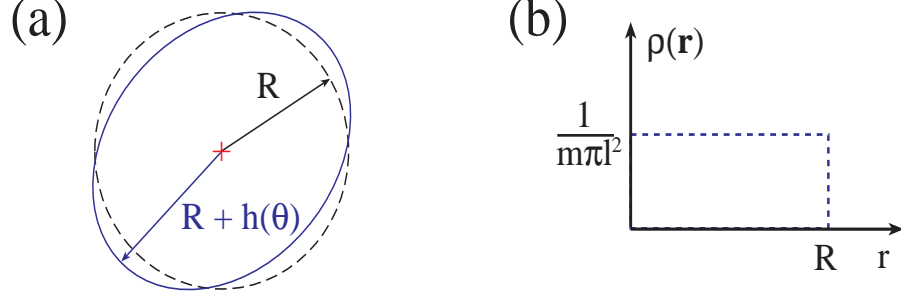


FIG. 3: (a) Deformation of the droplet boundary and (b) semiclassical approximation to the ground state density profile.

Following Wen [19], we develop an effective low-energy description for a finite droplet of $\nu = \frac{1}{m}$ -Laughlin liquid. Henceforth, we shall consider only the Hamiltonian in the rotating frame. However, when computing physical properties we shall transform to the laboratory frame (see Appendix A for details of how this transformation must be performed). In the ground state, the shape of the droplet is circular, and the density will be taken to be uniform and equal to $\rho_o = N/A$, $A = \pi R^2$ being the area of the droplet (see Fig. 5). We find A by noticing that if Φ_m is expanded in powers of, say, z_1 , the highest power is $l_{\max} = m(N-1)$, which corresponds to the angular momentum of the highest occupied single-particle orbital in the LLL. The extent of this orbital gives the radius of the droplet, $R = l_{\max}^{1/2} \ell \approx (mN)^{1/2} \ell$; hence $\rho_o = 1/(m\pi \ell^2)$ for $N \gg 1$. Next, imagine a deformation of the droplet such that the boundary is shifted to $R + h(\theta)$ for $0 \leq \theta < 2\pi$. Clearly, since this is a low-energy description the deformation must be small: $h(\theta) \ll R$. In addition, our hydrodynamic description necessarily breaks down at the scale of the oscillator length ℓ . This implies that $h(\theta) \gg \ell$ or, in terms of angular momentum of the excitations, the effective theory will be valid for modes with angular momentum $\lesssim \hbar \sqrt{mN}$.

In what follows, we work with the particle density per unit angle (sometimes we shall call it *current* because it is proportional to it),

$$j(\theta) = \rho_o R h(\theta). \quad (9)$$

Let us write down the energy cost (i.e. the Hamiltonian) for a deformation of the droplet, being $v(\mathbf{r}) = M(\omega_\perp^2 - \Omega^2) \mathbf{r}^2/2$, the confining potential in the rotating reference frame (cf. Eq. (2)), and $\mu \equiv v(|\mathbf{r}| = R)$, the chemical potential. The appropriate expressions read:

$$H = \int d^2 \mathbf{r} (v(\mathbf{r}) - \mu) [\rho(\mathbf{r}) - \rho_o(r)] = \frac{FR\rho_o}{2} \int_0^{2\pi} d\theta h^2(\theta) = \frac{F}{2\rho_o R} \int_0^{2\pi} d\theta j^2(\theta), \quad (10)$$

where $\rho_o(r) = \rho_o \theta(R-r)$ and $F = v'(R)$. We will allow for the possibility that the deformation involves the addition or removal of a small number $Q = \int_0^{2\pi} d\theta j(\theta) \ll N$ of particles at the boundary. Canonical quantization of (10) can be achieved with the help of the continuity equation,

$$\partial_t j(l, t) = i\nu l j(l, t), \quad (11)$$

which has been expressed in terms of the Fourier modes of $j(\theta) = \sum_l j(l) \exp(-il\theta)/2\pi$. Notice that, contrary to the case of single-particle orbitals, in this case l measures, not the absolute angular momentum of the excitation, but the increase in the angular momentum over the ground state. The quantized effective Hamiltonian takes the form

$$H = \hbar \nu m \sum_{l>0} j(l) j(-l) + \frac{\hbar \nu}{2} m Q^2. \quad (12)$$

The canonical commutation relations lead to the following *current algebra*: $[j(l), j(l')] = \frac{l'}{m} \delta_{l+l', 0}$, which in the mathematical Physics literature is known as U(1) Kac-Moody (KM) algebra. Nevertheless, both the Hamiltonian

and the current algebra can be written in a more familiar way if, for $l > 0$, we introduce $b(l) \equiv -i\sqrt{\frac{m}{l}} j(-l)$ and $b^\dagger(l) \equiv i\sqrt{\frac{m}{l}} j(l)$; hence $[b(l), b^\dagger(l')] = \delta_{l,l'}$, i.e. the familiar “phonon” algebra. In terms of these operators

$$H = \sum_{l>0} \hbar v l b^\dagger(l) b(l) + \frac{\hbar v}{2} m Q^2, \quad (13)$$

i.e. the Hamiltonian of a system of *chiral* phonons with energy dispersion $\hbar v l$ ($\hbar \omega_\perp l$ in the laboratory frame). Therefore, the spectral degeneracies are given by $p(l)$. The chirality of surface modes stems from the broken time-inversion symmetry existing in this situation: The system rotates in one direction, which is reversed under time inversion. Furthermore, it is also important to point out that the state annihilated by the $b(l)$ operators must be the Laughlin state. This is related to the existence, *in the rotating frame*, of a finite energy gap which must be overcome in order to decrease the angular momentum below that of the Laughlin state, and should be interpreted as due to the incompressibility of the Laughlin state (i.e. the droplet cannot further shrink) [33]. Thus we conclude that the effective theory correctly describes all the features of the low-energy spectrum obtained using wave functions.

The first property that we want to compute using the effective theory is the response to a weak time-dependent deformation of the trapping potential. This couples to the particle density at the boundary, and therefore to $j(\theta)$ (see appendix A for more details). The measurable response will be given in terms of the dynamic structure factor,

$$S_{ROT}(l, \omega) = \int_{-\infty}^{+\infty} dt e^{i\omega t} \int_0^{2\pi} d\theta e^{-il\theta} \langle j(\theta, t) j(0, 0) \rangle, \quad (14)$$

where the brackets stand for thermal average over the canonical ensemble in the rotating frame, which is where the system is in thermal equilibrium. The above function can be written in terms of the response to an external potential, by virtue of the fluctuation-dissipation theorem [39]. At a temperature T , the relationship is given by

$$S_{ROT}(l, \omega) = \frac{2\hbar \text{Im } \chi(l, \omega)}{(e^{-\hbar\omega/T} - 1)}, \quad (15)$$

where $\chi(l, \omega)$ is the Fourier transform of

$$\chi(\theta, t) = -\frac{i}{\hbar} \vartheta(t) \langle [j(\theta, t), j(0, 0)] \rangle, \quad (16)$$

where $\vartheta(t)$ is the step function. The previous correlation function can be readily computed using current algebra described above and the continuity equation, which implies that $j(\theta, t) = j(\theta - vt)$. Thus, applying the results of appendix A, we arrive at the following result for the dynamic structure factor in *laboratory* frame:

$$S_{LAB}(l, \omega) = S_{ROT}(l, \omega - l\Omega) = \frac{l}{m} \frac{\delta(\omega - \omega_\perp l)}{1 - e^{-\hbar(\omega_\perp - \Omega)l/T}}. \quad (17)$$

Since there is a single branch of phonons, the fact that $S_{LAB}(l, \omega)$ is peaked at $\omega = \omega_\perp l$ should not be surprising (in real systems, a finite broadening of the peak is expected). However, it is also important to notice that the spectral weight of the peak associated with the surface mode (cf. Eq. (17)) is proportional to the filling fraction $\nu = 1/m$ of the Laughlin state.

A way to understand the proportionality to the filling fraction of the spectral weight is to show that, as far as the response to an external potential is concerned, a droplet of Laughlin liquid behaves as a rapidly rotating cloud of non-interacting particles (i.e. an ideal gas) with *peculiar exclusion statistics* [24]. To understand what this means, let us assume that when the ideal gas is in thermal equilibrium it is described by a density matrix ρ^0 such that $\rho^0|k\rangle = N(k)|k\rangle$. The function $N(k)$ is the occupancy of a single-particle orbital $|k\rangle$ with angular momentum equal to $\hbar k$. To compute the *linear* response of this ideal gas to the external perturbation $\delta v_{ext}(\theta, t)$ localized near the boundary, let us consider the linearized equation of motion for the perturbed density matrix $\rho^0 + \delta\rho(t)$,

$$i\hbar \langle k+l | \partial_t \delta\rho(t) | k \rangle = \langle k+l | [H_0, \delta\rho(t)] + [\delta v_{ext}(\theta, t), \rho^0] | k \rangle. \quad (18)$$

where $H_0|k\rangle = \varepsilon(k)|k\rangle$, $\varepsilon(k) = \hbar v k$ being the single-particle dispersion. We thus find ($\eta \rightarrow 0^+$):

$$\chi(l, \omega) = \lim_{\delta v_{ext} \rightarrow 0} \frac{\delta \langle j(l, \omega) \rangle}{\delta v_{ext}(l, \omega)} = \frac{1}{2\pi\hbar} \sum_k \frac{N(k) - N(k+l)}{\omega - (\varepsilon(k+l) - \varepsilon(k)) / \hbar + i\eta}. \quad (19)$$

Since the particles have been assumed to be non-interacting we can use the results of Sect. II, which imply that the single-particle dispersion is *linear* with the angular momentum. Thus the previous expression reduces to

$$\chi(l, \omega) = \frac{1}{2\pi\hbar} \frac{1}{\omega - \nu l + i\eta} \sum_{k=0}^{+\infty} [N(k) - N(k+l)] = \frac{g^{-1}}{2\pi\hbar} \frac{1}{\omega - \nu l + i\eta}. \quad (20)$$

It is important to stress that the above expressions make sense as long as $l \ll \sqrt{mN}$, otherwise the effect of the external potential is not reduced to the neighborhood of the boundary and radial part of the single-particle orbitals must be taken into account. In the previous expression we have denoted as g^{-1} the mean occupancy at the bottom of the single-particle band (cf. Fig. 2), which at the low temperatures where the gas is quantum degenerate must be a constant. By comparing this expression for $\chi(l, \omega)$ with the one obtained from the effective theory, we arrive at the identification $g = m = 2$, which implies that at the bottom of the band the mean occupancy is $\frac{1}{2}$. This may seem surprising, as it means that near the bottom of the band there is one particle per two states, a situation that does not correspond to neither fermions ($g = 1$) nor bosons ($g = 0$) [24]. However, we can argue that this result makes indeed sense. Let us first emphasize that we have assumed that the droplet is an ideal gas, which seems to be at odds with the fact that the actual particles (i.e. the bosons) are interacting. However, we must remember that under the combined action of interactions and rapid rotation, the bosons effectively become *hard-core* so that their many-body wave function has zero interaction energy. This pushes the atoms to orbits where their relative angular momentum is equal to $2\hbar$. As a result, there is, on average, one boson per every two angular momentum states: We have N particles in the states from $l = 0$ to $l_{max} = 2(N - 1)$, i.e. in $2N - 1$ states, which for $N \gg 1$ yields two states per particle. Therefore, the rapid rotation plus interactions become a “statistical” interaction, which makes the bosons behave as if they are non-interacting “super-fermions” obeying Haldane’s *exclusion* statistics [24, 29, 30] with $g = 2$. Going back to our discussion of the experimental characterization of the Laughlin state, we have thus shown that the appearance of the filling fraction in the spectral weight of $S_{LAB}(l, \omega)$ can be interpreted as an sign of the peculiar statistical aspects of the Laughlin liquid. Therefore, if one measured the spectral weight of $S_{LAB}(l, \omega)$ and found it to be proportional to $\frac{1}{m}$, this would provide a fairly direct evidence for the fact that exclusion statistics is at play in the Laughlin state [30, 31].

Another function of experimental interest is the one-body density matrix. To compute it, one needs to find a representation for the bosonic field operator at the boundary. To this purpose, it will be convenient to introduce the phonon field $\phi(\theta)$, related to the density $j(\theta)$ by $\partial_\theta \phi(\theta) = 2\pi j(\theta)$. Expanding it in normal modes:

$$\phi(\theta) = \frac{\phi_0}{m} + Q\theta + \frac{1}{\sqrt{m}} \sum_{l>0} \frac{1}{\sqrt{l}} [e^{il\theta} b(l) + e^{-il\theta} b^\dagger(l)], \quad (21)$$

with $[Q, \phi_0] = i$. In order to construct an operator with the same properties as the boson field operator, we first notice that if a boson is added at θ_0 , the density $j(\theta)$ becomes $j(\theta) + \delta(\theta - \theta_0)$. By direct calculation using (21), one can check that $[j(\theta), \phi(\theta')] = \frac{i}{m} \delta(\theta - \theta')$, which means that $j(\theta)$ and $m\phi(\theta)$ are canonically conjugate to each other. Thus the operator that we seek must be proportional to $e^{-im\phi(\theta)}$, since $e^{im\phi(\theta_0)} j(\theta) e^{-im\phi(\theta_0)} = j(\theta) + \delta(\theta - \theta_0)$. In this construction, the boson appears as a *soliton* or *kink* in the field $\phi(\theta)$ with topological charge $Q = +1$. Fractionally charged excitations can be also constructed, though they are not physical boundary excitations for the droplet geometry. They are created by the operator $e^{-i\phi(\theta_0)}$, which shifts $j(\theta) \rightarrow j(\theta) + \frac{1}{m} \delta(\theta - \theta_0)$ and therefore describes the creation of a quasi-particle at $z_0 \approx R e^{i\theta_0}$. One important consistency test, before we proceed any further, is to show that the putative boson operator, and its hermitian conjugate, are commuting at different points. For $\theta \neq \theta'$, we have that

$$\begin{aligned} e^{im\phi(\theta)} e^{\pm im\phi(\theta')} &= e^{\mp m^2 [\phi(\theta), \phi(\theta')]} e^{\pm im\phi(\theta')} e^{im\phi(\theta)} \\ &= (-1)^m e^{\pm im\phi(\theta')} e^{im\phi(\theta)}, \end{aligned} \quad (22)$$

and $(-1)^m = +1$ since $m = 2$. Indeed, by repeating this calculation with m replaced by ν^{-1} , one can see that commuting fields are obtained *only* when $\nu^{-1} = m$ is an even integer (if m is odd, the fields anti-commute, and this is the situation usually encountered in the FQHE, where the constituents are electrons). Wen has argued [19] that for $\nu \neq 1/m$, there must be more than one phonon branch in the spectrum, otherwise no field operator can be constructed and the effective theory is not self-consistent. Below, we shall give explicit examples of how the additional branches appear. To close this part of the discussion, it is worth mentioning that the *exchange* statistics of the excitations created by $e^{-i\phi(\theta)}$ is fractional, since $e^{-i\phi(\theta)} e^{-i\phi(\theta')} = e^{-i\pi \text{sgn}(\theta - \theta')/m} e^{-i\phi(\theta')} e^{-i\phi(\theta)}$. That is, after exchanging two boundary quasi-particles we pick up a phase factor equal to $\pm\pi/m = \pm\pi/2$. These excitations are $\frac{1}{2}$ -anyons.

The complete form of the (boundary) field operator in terms of the phonon field is

$$\Psi^\dagger(z = R e^{i\theta}) \equiv \Psi^\dagger(\theta) = A e^{-im[l_0\theta + \phi(\theta)]}, \quad (23)$$

where A is a constant that depends on the way the modes at high $l \gtrsim \sqrt{mN}$ are excluded from the above sums. The value $l_o = (N - \frac{1}{2})$ is obtained by comparing with the spectral representation of the one-body density matrix, Eq. (24). Calculation of the one-body density-matrix at the boundary is now possible using (21) and (23):

$$G(\theta) = \langle \Psi^\dagger(\theta) \Psi(0) \rangle = e^{-iml_o(\theta-\theta')} \langle e^{-im\phi(\theta)} e^{im\phi(0)} \rangle. \quad (24)$$

This function has two interesting limits ($\theta \gg \ell/R$ in both cases). When the temperature is higher than the phonon

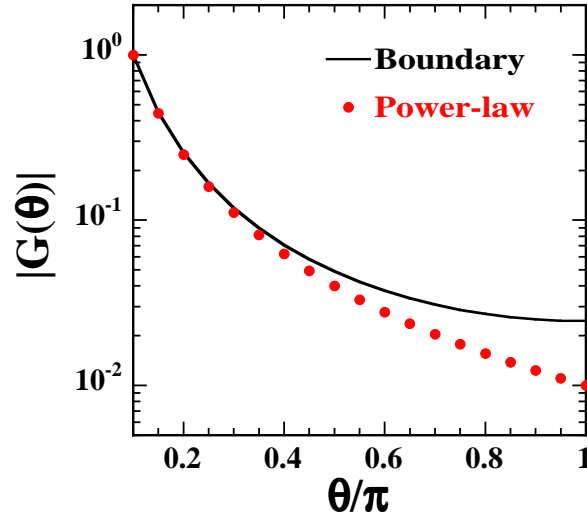


FIG. 4: Behavior of the density matrix at the boundary compared with the power-law $1/\theta^2$. The functions have been normalized to 1 at $\theta = 0.1\pi$. The power-law decay is accurately followed for small angles, whereas for large angles $|G(\theta)|$ decays more slowly since it is periodic on a finite-length boundary. In this respect, notice that $|G(\theta)|$ has reflection symmetry about $\theta = \pi$.

level spacing, i.e. if $T \gg \hbar v$, then

$$G(\theta) = \text{const.} \times \left(\frac{\pi T}{\hbar v} \right)^m e^{-iml_o\theta} \left[\sinh \left(\frac{\pi T \theta}{\hbar v} \right) \right]^{-m}, \quad (25)$$

and therefore correlations decay exponentially at large θ , but have power law form at small θ . In the more demanding temperature regime where $T \ll \hbar v$, the density matrix reads:

$$G(\theta) = \text{const} \times e^{-iml_o\theta} \left[\sin \left(\frac{\theta}{2} \right) \right]^{-m}, \quad (26)$$

and exhibits an “almost power-law” behavior with θ (see Fig. 4), which is cut off by the finite length of the boundary. The last form, Eq. (26), has been numerically shown to be accurate for a system of $N = 36$ bosons by Lee and Wen [33] (see also Ref. 34 for $m = 3$ calculations). It is interesting to compare Eq. (26) with the one-body density matrix away from the boundary [35],

$$G(\mathbf{r}, \mathbf{r}') = \frac{1}{m\pi\ell^2} e^{-|z-z'|^2/2\ell^2} e^{(z^*z' - z'^*z)/2\ell^2}. \quad (27)$$

Apart from the last term, which is a phase factor, it can be seen that this function decays at large distances as a gaussian. This is in contrast to the almost-power-law decay that the same function exhibits near the boundary, where $|\mathbf{r}| \approx |\mathbf{r}'| \approx R$. The differences in behavior are due to the *quantum critical* fluctuations of the surface modes.

Nevertheless, it seems difficult that the behavior of density matrix near the boundary, Eq. (26), can be experimentally measured. This is because for a small droplet any measurement of the one-body correlation function would be

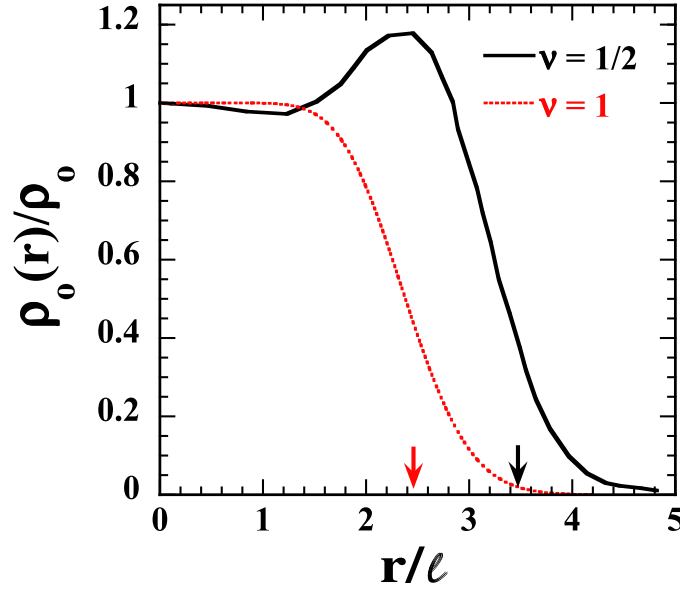


FIG. 5: Density profile of the $\nu = 1$ and $\nu = \frac{1}{2}$ Laughlin states for $N = 6$ particles. The latter corresponds to boson and the former to fermions. The density is normalized to the bulk values $\rho_0 = 1/\pi\ell^2$ for the $\nu = 1$ and $\rho_0 = 1/2\pi\ell^2$ for $\nu = \frac{1}{2}$. Notice that the $\nu = \frac{1}{2}$ state is more extended than the $\nu = 1$. The arrows indicate the position of the semiclassical radius $R = \sqrt{mN}\ell$. Data for the $\nu = \frac{1}{2}$ state has been taken from Ref. 18.

dominated by the bulk signal coming from (27). However, it turns out that the result (26) does have some effect on the density profile. To see this, we first notice that Eq. (26) can be written using the binomial expansion as

$$G(\theta) = \text{const.} \times \sum_{p=0}^{+\infty} \frac{(p+m-1)!}{p!(m-1)!} e^{i(p-l_{max})\theta}, \quad (28)$$

from which the occupancy of the levels near l_{max} can be obtained:

$$\langle n(l) \rangle \propto \int_0^{2\pi} d\theta G(\theta) e^{il\theta} \quad (29)$$

with $l = 0, 1, \dots$. Thus we find [19] that, for $l \leq l_{max}$,

$$\langle n(l) \rangle = \text{const.} \times \frac{(l_{max} - l + m - 1)!}{(l_{max} - l)!(m - 1)!} \quad (30)$$

and vanishes for $l > l_{max}$, as expected. Therefore, for $m = 2$, the occupancy near the boundary behaves as $(l_{max} + 1 - l)$. But given the limitations of the effective theory, this result will valid for $(l_{max} - l) < \sqrt{mN}$. Mitra and MacDonald [42] computed $\langle n(l) \rangle$ numerically for small Laughlin droplets with $m = 3, 5, 7$ and found good agreement with the general expression, Eq. (30), within its validity range. Moreover, they also found that $\langle n(l) \rangle$ exhibits a prominent peak followed by smaller oscillations as l decreases from l_{max} to 0, i.e. as one moves from the boundary to the center of the droplet. For large enough droplets, the oscillations eventually damp out as $\langle n(l) \rangle$ approaches, rather slowly, the average value of $\frac{1}{m}$. This behavior can be understood on the basis of two facts: i) The existence of a cut-off at zero temperature, for $l = l_{max}$, above which $\langle n(l) \rangle$ vanishes according to Eq. (30) (e.g. as $(l_{max} + 1 - l)$ for $m = 2$), and ii) the fact that the average occupancy equals $\frac{1}{m}$ ($= \frac{1}{2}$ in the present case). These two facts imply that as l approaches l_{max} from below, the occupancy must necessarily *decrease* below the average $\frac{1}{2}$. However, to maintain the average occupancy, the particles removed from the neighborhood of l_{max} must be placed in orbitals with lower angular momentum. Since for relatively large droplets, $\langle n(l) \rangle \approx \frac{1}{m}$ for $l \ll l_{max}$, it seems reasonable to expect that $\langle n(l) \rangle$ exceeds the average by displaying a maximum before it decays to zero as required by Eq. (30). As the orbitals with l quanta of angular momentum are located around $r_l \sim \ell\sqrt{l}$, the peak in $\langle n(l) \rangle$ translates into a peak in the density near the boundary. This can be observed in Fig. 5, where the density profile of a $\nu = \frac{1}{2}$ Laughlin droplet with

$N = 6$ particles has been plotted. The density is related to $\langle n(l) \rangle$ by the following expression,

$$\rho_o(\mathbf{r}) = \sum_{l=0}^{l_{max}} \langle n(l) \rangle |\varphi_l(\mathbf{r})|^2. \quad (31)$$

This result is a consequence of the Laughlin state being an eigenstate of the total angular momentum. When summing over l , the occupancy at angular momentum $\hbar l$ is averaged over the neighboring orbitals, and in the present case any oscillations displayed by $\langle n(l) \rangle$ are washed out. The density near the center of the trap reaches the constant value of $1/(2\pi\ell^2)$, which corresponds to the average occupancy $\frac{1}{2}$. Nonetheless, a peak in the density near the boundary appears and should be visible in an experiment where the density profile is measured. In this respect, it was shown in Ref. [21] using Eq. (31) that by turning the trapping potential off and allowing the atoms to expand freely, the density profile of a vortex liquid expands self-similarly. This fact can be used to perform very accurate measurements of the density profile, which should reveal a characteristic peak near the boundary for the Laughlin state (and possibly for other vortex liquids), and which is not expected for Bose-condensed systems.

For comparison purposes, in Fig. 5 we have also plotted the density profile for the fermionic $\nu = 1$ Laughlin state. This is a state where particles are non-interacting, and the occupancy is known exactly: $\langle n(l) \rangle = 1$ for $l \leq l_{max} = N-1$, and zero for $l > l_{max}$. This is again in agreement with (30), which predicts $n(l) = \text{const.}$, for $l \leq l_{max}$ (this constant cannot be fixed by the effective theory). In this case $\langle n(l) \rangle$ vanishes abruptly for $l = l_{max} + 1$. Therefore, we do not expect a peak in the density near the boundary. We conclude that the peak is a consequence of the strong correlations built into the Laughlin state. It is indeed a generic property of finite droplets of the Laughlin liquid, and in a more general framework is a particular example of the generalized Luttinger's theorem [41] discussed by Haldane in Ref. 46.

We end this section by emphasizing the fundamental difference between the boson occupancy, $\langle n(l) \rangle$, and the occupancy for the ideal “super-fermion” gas, $N(l)$, introduced in our discussion of the density response of the Laughlin droplet. The latter is a convenient tool, which can be also used to discuss some other properties of the Laughlin liquid, e.g. the thermodynamics of the boundary excitations or the Hall conductance [31]. The boson occupancy $\langle n(l) \rangle$ contains in addition correlation effects between the actual particles, which lead, for instance, to the almost power-law behavior of $G(\theta)$. A mathematically rigorous discussion of these issues can be found in Ref. 31.

IV. OTHER STABLE STATES OF SCALAR BOSONS

The Laughlin state described in the previous section has the property of being an exact eigenstate of the Hamiltonian:

$$H = \sum_{i=1}^N H_i + g_{2d} \sum_{i < j=1}^N \delta(\mathbf{r}_i - \mathbf{r}_j). \quad (32)$$

More precisely, (8) is the state with the lowest energy for $L = \hbar m N(N-1)/2$. On the other hand, the states that we will consider in this section are not exact eigenstates of (32). They have been obtained numerically using two different types of exact diagonalization set-ups. If one is only interested in the bulk properties of vortex liquids, and taking into account that exact diagonalization is only feasible with relatively small particle numbers, the Hamiltonian can be efficiently diagonalized on a *compact* manifold, like a torus [5] or a sphere [6]. Cooper *et al.* used the toroidal geometry to study the stability of the Abrikosov lattice as the filling fraction $\nu = N/N_v$ (N_v being the number of vortices) is varied. They found that the lattice melts for $\nu \sim 6$ and that for smaller filling fractions a rotating bosonic system exhibits a series of gapped states (*homogeneous* vortex liquids) when ν belongs to the sequence $\frac{1}{2}, 1, \frac{3}{2}, 2, \dots, \frac{5}{2}, \dots$. The gap is a signature of the incompressibility of the vortex liquid. The $\nu = \frac{1}{2}$ state was found to correspond to the Laughlin state discussed above, while the remaining states were shown to have good overlap with the Moore-Read state (for $\nu = 1$, see below) and other wave functions of the class introduced by Read and Rezayi [27]. At the same time, the Laughlin and Moore-Read states had been previously found in another type of exact diagonalization studies [10, 11] where the bosons are confined by a harmonic potential. This is a situation that is closer to the one experimentally relevant, and in which the vortex liquids are *inhomogeneous*. In this set-up, Cooper and Wilkin [10] found a series of stable states at magic values of the total angular momentum, L . The series terminates at the $\nu = \frac{1}{2}$ -Laughlin state, and many of the remaining stable states have good overlap with wave functions constructed from the following ansatz:

$$\Phi_B^{(n)}(z_1, \dots, z_N) = \mathcal{P}_{LLL} \left[\Phi_1(z_1, \dots, z_N) \Phi^{(n)}(\mathbf{r}_1, \dots, \mathbf{r}_N) \right], \quad (33)$$

where $\Phi_1 = \Phi^{(1)}$ denotes the Jastrow factor, $\prod_{i < j} (z_i - z_j)$, and $\Phi^{(n)}$ is a Slater determinant representing the state of N fictitious fermions, the so-called “composite fermions” (CF's), distributed over n Landau levels. The operator

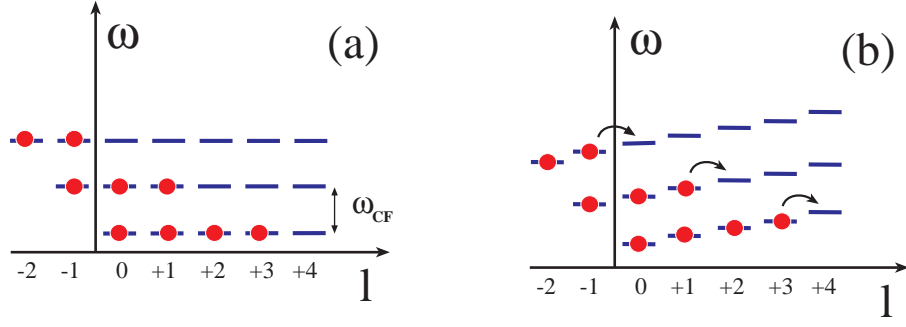


FIG. 6: A compact state with $N = 9$ composite fermions (a and b), which corresponds to the integer sequence $[4, 3, 2]$. In (b) we have represented the effect of the confinement, which is to lift the degeneracy of the otherwise degenerate levels within every CF Landau level. Surface excitations can be pictured as low-energy particle-hole excitations (b) within each Landau level. For these excitations the composite fermions can be weakly interacting, even if the interactions could be neglected in the ground state.

\mathcal{P}_{LLL} is needed to project the ansatz onto the LLL (for details of how this projection should be carried see Ref. 5 and Ref. 30). Furthermore, Cooper and Wilkin found that the stable states are “compact”, a term coined by Jain and Kawamura [28] to refer to those states where N_i CF’s occupy the lowest angular momentum orbitals in the i -th CF Landau level ($i = 0, 1, \dots, n-1$, so that $\sum_{i=0}^{n-1} N_i = N$, see Fig. 6). Therefore, a compact state is characterized by the set of integers: $[N_0, N_1, N_2, \dots, N_{n-1}]$, and it has an energy equal to $\hbar\omega_{CF} \sum_{i=0}^{n-1} N_i(i + \frac{1}{2})$, where $\omega_{CF} = \omega_{CF}(N)$ is the effective CF Landau level spacing [10, 28]. However, it is necessary to stress that not all compact CF states are stable [28]. In the large N limit, the CF ansatz yields *homogeneous* vortex liquids whose filling fraction falls into the *bosonic* Jain sequence [5], i.e. $\nu = n/(n+1)$ or $\nu = (n+1)/n$, for an integer $n \geq 1$. Except for the $\nu = \frac{1}{2}$ -Laughlin state, this sequence does not match the one found by Cooper *et al.* using the toroidal geometry, and this has led to some confusion. The situation has been recently clarified by Regnault and Jolicoeur [6] who performed exact diagonalizations on another compact geometry, namely a sphere, and checked for the convergence of the spectral gap with the system size. They found the existence of stable homogeneous vortex liquids for $\nu = \frac{1}{2}, \frac{2}{3}, \frac{3}{4}, \frac{4}{3}, \frac{5}{4}$, falling into to the Jain sequence, and for $\nu = 1$, which corresponds to the Moore-Read state. Therefore, below we shall consider the surface modes of some of the states in the Jain sequence as well as the Moore-Read state.

To study the surface waves of the vortex liquids whose wave functions can be obtained from the CF ansatz, Eq. (33), we will employ the *parton* construction [19, 37]. Usually, this method assumes that the number of particles, N , is macroscopically large so that the inhomogeneity of the system can be neglected. For these states, one can safely assume that there are n CF Landau levels filled by N/n composite fermions. As pointed out above, the resulting state is characterized by a filling fraction $\nu = n/(n+1)$. However, when dealing with a *mesoscopic* droplet, this is not necessarily true and the compact states exhibiting good overlap with the stable states usually have *unequal* number of CF in different Landau levels. Generalizing the parton construction for this situation is not difficult, the only limitation being imposed by the subsequent use of the effective low-energy theory introduced in Sect. III to describe of the surface waves of a given CF Landau level, i . This requires that the CF level occupancy $N_i \gg 1$, which is not always fulfilled. Nevertheless, it was found [36] that having some of the higher CF Landau levels occupied with $N_i \sim 1$ CF’s corresponds to quasi-particle excitations over a state of the Jain hierarchy. Therefore, these states can be characterized by an effective number of CF levels to which the effective theory can be applied. In the discussion that follows, we denote this number by $p (\leq n)$. In other words, this integer, which yields the *effective* filling fraction $\nu = p/(p+1)$, can be associated with the number of CF Landau levels with occupancy $N_i \gg 1$.

Keeping in mind the above caveats, we can regard the CF ansatz (33) as describing a bound state, the fundamental boson, made up of *two* kinds of fermions (called “partons”) such that the many-body wave function (we drop \mathcal{P}_{LLL} for notational simplicity) reads:

$$\Phi_B^{(n)}(z_1, \dots, z_N) = \Phi_1(z_1^{(1)}, \dots, z_1^{(1)}) \Phi^{(n)}(z_1^{(2)}, \dots, z_N^{(2)}) \Big|_{\{z_i^{(1)} = z_i^{(2)} = z_i\}_{i=1, \dots, N}}. \quad (34)$$

Thus a boson is a type-1 parton in the (fermion) LLL, which carries a “charge” $q_1 = p/(p+1)$, bound to a second parton (type-2), which carries charge $q_2 = 1/(p+1)$ so that $q_1 + q_2 = 1$. Type-1 has one branch of boundary excitations, whereas type-2 partons contribute with $p \leq n$ branches corresponding to the p CF levels with $N_i \gg 1$ (to see how this comes about, repeat the steps that lead to the effective theory, now setting $m = 1$ for type-1 partons, and considering p different branches with $m = 1$ for type-2 partons). However, not all of these $p+1$ branches are independent. In

fact, the bound state condition implies that the density of type-1 partons cannot fluctuate independently of that of type-2 partons. Therefore, we must demand that all *physical* operators do not excite density fluctuations where both partons behave independently. Mathematically, if O is a physical operator, then $[\rho_c, O] = 0$, with $\rho_c = \rho_0 - \sum_{i=1}^p \rho_i$, where ρ_0 describes the surface modes of type-1 partons, and ρ_i for $i = 1, \dots, p$ those of type-2. These operators obey the current algebra:

$$[\rho_i(l), \rho_j(l')] = l' \delta_{l+l',0} \delta_{i,j}. \quad (35)$$

As mentioned previously, there are p independent branches, which are obtained by requiring the currents to be physical operators, in the sense introduced above. Thus it is found that one of the independent currents corresponds to the total current $j_0 = q_1 \rho_0 + q_2 \sum_{i=1}^p \rho_i$, and the remaining $p-1$ are given by $j_i = \sum_{j=1}^p a_{ij} \rho_j$ ($i = 1, \dots, p-1$), where a_{ij} are $p-1$ orthogonal vectors such that $\sum_{j=1}^p a_{ij} = 0$.

To illustrate how the parton construction works in practice, we first notice that one can readily recover the results of Sect. III for the surface waves of the $\nu = \frac{1}{2}$ Laughlin state, which in the present context corresponds to setting $p = n = 1$. However, a less straightforward exercise is provided by a state where $p = 2$ (and $\nu = \frac{2}{3}$ effectively). Using the parton construction, we find that there are *two* independent branches of surface modes, described by the currents $j_0 = (2\rho_0 + \rho_1 + \rho_2)/3$, and $j_1 = \rho_1 - \rho_2$, respectively, which obey

$$[j_0(l), j_0(l')] = \frac{2}{3} l' \delta_{l+l',0}, \quad (36)$$

$$[j_1(l), j_1(l')] = 2l' \delta_{l+l',0}. \quad (37)$$

As a check, it is worth trying to obtain these results from a different point of view. Let us first recall that the $\nu = \frac{2}{3}$ state can be obtained by means of the hierarchical construction [38] where the state at $\nu = 2/3$ can be thought of as two component vortex liquid, containing one liquid with $\nu_0 = \frac{1}{2}$, which corresponds to the *parent* Laughlin state, and another one with $\nu_1 = \frac{1}{6}$, which corresponds to a Laughlin state of quasi-particles over the parent state of bosons. Notice that the sum of filling fractions $\nu_0 + \nu_1 = \nu$. If, for the moment, we neglect any interactions between the two components of the liquid, the effective theory can be used to describe each one separately. This leads to the following current algebra:

$$[\sigma_0(l), \sigma_0(l')] = \frac{1}{2} l' \delta_{l+l',0}, \quad (38)$$

$$[\sigma_1(l), \sigma_1(l')] = \frac{1}{6} l' \delta_{l+l',0}, \quad (39)$$

where σ_0 describes the boundary phonons of the $\nu_0 = \frac{1}{2}$ liquid and σ_1 those of the $\nu_1 = \frac{1}{6}$ liquid.

To find the relationship between the parton currents and the currents σ_0 and σ_1 , we resort to the interpretation of j_0 as the total current. This implies that $j_0 = \sigma_0 + \sigma_1$. The other current must be an independent linear combination, which is readily found to be $j_1 = \sigma_0 - 3\sigma_1$. This, quite direct, identification of the currents helps to confirm the results obtained from the parton construction. Thus we conclude that, just as we briefly remarked in Sect. III, for states other than the Laughlin states there are several branches of surface modes. In particular, for the compact CF states considered above, there can be $p > 1$ branches.

Let us finally turn our attention to the dynamic structure factor for the states considered above. As it was pointed out previously, these states are not exact ground states of the Hamiltonian, which means that we cannot use the wave function approach of Sect. III to get much insight into the excitation energy of the surface modes. Furthermore, the non-interacting CF picture may only hold to describe the ground states but not their low-lying excitations. In other words, some small residual interactions are always expected. However, if we start by assuming that the non-interacting CF holds, then the energy of the surface modes will be just the confinement energy, and therefore the Hamiltonian reads:

$$H_o = \hbar \pi \nu \sum_{\alpha=0}^{p-1} \int_0^{2\pi} d\theta J_\alpha^2(\theta). \quad (40)$$

In the above expression we have normalized the p independent currents so that $[J_\alpha(l), J_\beta(l')] = l' \delta_{\alpha,\beta} \delta_{l+l',0}$ (notice that this normalization differs from the one used above for j_0 and j_i , $i = 1, \dots, n-1$). In the absence of interactions, the p phonon branches are all degenerate. However, since the potential $\delta v_{LAB}(\theta)$ (see appendix A) couples only to $j_0(\theta) = \sqrt{\nu} J_0(\theta)$ (where $\nu = p/(p+1)$), $S_{LAB}(l, \omega)$ will have the form (17), displaying a single peak at $\omega = \omega_\perp l$, but with $p/(p+1)$ replacing $1/m$ or, in other words, with total spectral weight *proportional* to $p/(p+1)$.

The spectrum is modified, however, if the residual interactions could not be neglected. In this case, one has to consider the effect of adding to the Hamiltonian terms like:

$$H' = \hbar\pi \sum_{\alpha,\beta=0}^{p-1} \int_0^{2\pi} \Delta v_{\alpha\beta} J_{\alpha}(\theta) J_{\beta}(\theta), \quad (41)$$

where $\Delta v_{\alpha\beta}$ is a real symmetric matrix. One could also have included terms containing derivatives of the currents, such like $g_{\alpha\beta} \int d\theta J_{\alpha}(\theta) \partial_{\theta} J_{\beta}(\theta)$. Other terms containing more than two current operators are also possible, and describe inelastic scattering processes among the surface phonons. Being *irrelevant* in the renormalization-group sense, these terms yield corrections to the energy of the surface modes of the order of $l(l/\sqrt{mN})^i$, where the index i equals the order of the current derivatives plus the number of current operators minus two (e.g. $i = 1$ in the previous example containing two currents and one derivative). These corrections can be important for modes with $l \sim \sqrt{N}$. To the lowest order in this case, however, the “normal” (surface) modes can be obtained by diagonalizing the matrix

$$\mathcal{H}_{\alpha\beta} = v \delta_{\alpha\beta} + \Delta v_{\alpha\beta}. \quad (42)$$

Nevertheless, the overall shape of the spectrum is constrained by the generalized Kohn’s theorem discussed in appendix A. This theorem is a consequence of the decoupling of the center of mass motion from other degrees of freedom in harmonically trapped systems. Since we have assumed that this is the case throughout, it implies that the energy (in the laboratory frame) of the $l = 1$ mode is given by the *bare* trap frequency ω_{\perp} . Let us begin by considering the case where there is a single phonon branch, like in the the Moore-Read state to be discussed below. Kohn’s theorem implies that $\omega(l = 1) = \omega_{\perp}$. Any corrections arising from interactions will necessarily have to vanish for $l = 1$. For instance, we can think of a general form for the dispersion (in the laboratory frame) like $\omega(l) = \omega_{\perp} l + l \sum_{i=1}^{+\infty} \delta\omega_{int}^{(i)}(l-1)^i$, where $\delta\omega_{int}^{(i)} \ll \omega_{\perp}$. In the case where there is more than one branch, the situation is slightly more complicated. Then, in principle, after diagonalizing the matrix $\mathcal{H}_{\alpha\beta}$, not all the eigenvalues will be degenerate, which implies that for $l = 1$, to this order, there can be several modes with distinct energy. However, the energy of, at least, one of the modes (the Kohn mode, associated with the center of mass motion) is still fixed to ω_{\perp} (in the laboratory frame). Furthermore, an analysis of the oscillator strength based on Kohn’s theorem (see appendix A and below) shows that the Kohn mode exhausts the all the oscillator strength available, which in turn forces all the modes to be degenerate at $l = 1$. Thus, the general form of the dispersion of the *normal* modes is a generalization of the single-branch case: $\omega(l, \alpha) = \omega_{\perp} l + l \sum_{i=1}^{+\infty} \delta\omega_{int}^{(i)}(\alpha)(l-1)^i$, where $\alpha = 1, \dots, p$ is the branch index. This form assumes the frequencies to be real and thus neglects any imaginary parts arising from inelastic coupling of surface modes. However, this fact can be readily accounted for, although we expect *this* linewidth to be small for the low-lying modes, and zero for $l = 1$.

The implications of the previous discussion for the dynamic structure factor can be easily extracted. After expressing the total current $j_0 = \sqrt{\nu} J_0$ in terms of the normal modes, we find that $S_{LAB}(l, \omega)$ should exhibit the following structure

$$S_{LAB}(l, \omega) = \sum_{\alpha=1}^p \frac{l w_{\alpha} \delta(\omega - \omega(l, \alpha))}{1 - e^{-\hbar(\omega(l, \alpha) - \Omega l)/T}}. \quad (43)$$

From the current algebra for $j_0(l)$, it follows the following sum rule:

$$\sum_{\alpha=1}^p w_{\alpha} = \frac{p}{p+1}. \quad (44)$$

According to the above considerations, for $l = 1$ all the branches must be degenerate: $\omega(1, \alpha) = \omega_{\perp}$, and hence there is single peak of spectral weight proportional to $p/(p+1)$. For $l > 1$ more than one (but at most p) peak can exist, and given that for repulsive interactions the energy of the Kohn mode is a lower bound of the surface phonon energy, all the peaks should appear at frequencies higher than (or equal to) $\omega_{\perp} l$. However, since the interactions are weak, it may well happen that the shifts and splittings are very small and hard to resolve experimentally, and this would produce a single peak again. The total spectral weight associated with the surface modes must be again proportional to $p/(p+1)$, for integer $p \geq 1$. However, if the different peaks for $l > 1$ could be resolved, the individual spectral weight of each peak would be determined by the detailed form of the interactions between modes, which is not fixed by the present effective field theory.

We close this section by considering the surface modes of the Pfaffian or Moore-Read (MR) state. This is a state that cannot be constructed from the the composite-fermion ansatz, Eq. (33). As it was mentioned at the beginning of

the section, for $\nu = 1$ exact diagonalization studies on the torus [5] and the sphere [6] have found an incompressible state exhibiting a large overlap with the MR state, whose wave function reads:

$$\Phi_B^{MR}(z_1, \dots, z_N) = \mathcal{A} \left[\frac{1}{z_1 - z_2} \cdots \frac{1}{z_{N-1} - z_N} \right] \prod_{i < j=1}^N (z_i - z_j), \quad (45)$$

where $\mathcal{A}[\dots]$ means that the bracketed product must be anti-symmetrized as follows (N is assumed to be even):

$$\mathcal{A} \left[\frac{1}{z_1 - z_2} \cdots \frac{1}{z_{N-1} - z_N} \right] = \frac{1}{2^{N/2}(N/2)!} \sum_{P \in S_N} (-1)^P \frac{1}{z_{P(1)} - z_{P(2)}} \cdots \frac{1}{z_{P(N-1)} - z_{P(N)}}. \quad (46)$$

In the previous expression P is a permutation of $1, 2, \dots, N$ and $(-1)^P$ denotes its signature. For instance, if we consider $N = 4$ particles,

$$\mathcal{A} \left[\frac{1}{z_1 - z_2} \frac{1}{z_3 - z_4} \right] = \frac{1}{z_1 - z_2} \frac{1}{z_3 - z_4} - \frac{1}{z_1 - z_3} \frac{1}{z_2 - z_4} + \frac{1}{z_1 - z_4} \frac{1}{z_2 - z_3}. \quad (47)$$

Alternatively, the MR state can be written in the following way [5, 11]:

$$\Phi_B^{MR}(z_1, \dots, z_N) = \mathcal{S} \left[\prod_{(i < j) \in A} (z_i - z_j)^2 \prod_{(k < l) \in B} (z_k - z_l)^2 \right], \quad (48)$$

where \mathcal{S} symmetrizes the product of the two Laughlin $\frac{1}{2}$ states over all possible partitions of N particles into *two disjoint* subsets A and B having $N/2$ particles each. The second form, Eq. (45), shows perhaps more explicitly that the lower angular momentum of the MR is attained by having $N(N-1)/2 - N(N/2-1)/2 = (N/2)^2$ pairs of bosons in orbits with zero relative angular momentum. This is to be contrasted with the Laughlin state, Eq. (8), where *all* boson pairs have relative angular momentum equal to $2\hbar$. This means that in the MR some particles must necessarily interact, in order to reduce the total angular momentum, which for this state equals $N(N-2)/2$ for N even and $L = (N-1)^2/2$ for N odd. Wilkin and Gunn found in Ref. 11 that this state is also a good candidate to describe the stable state found for rotating bosons in a harmonic trap at $L = N(N-2)/2$ (for even N).

Surprisingly, the MR state becomes an exact eigenstate with zero interaction energy for a model where the particles interact by means of a repulsive three-body potential ($g_3 > 0$) [20]

$$V_3 = g_3 \sum_{i < j < k} \delta^{(2)}(\mathbf{r}_i - \mathbf{r}_k) \delta^{(2)}(\mathbf{r}_i - \mathbf{r}_j). \quad (49)$$

This follows from the property that MR vanishes when any three-particles come together, and has implications for the stability of the state with respect to three-body losses. We have previously found that the Laughlin state was a zero energy eigenstate of a two-body interaction potential. This is because its wave function vanishes as any two-particles approach each other, hence the probability for three particles to be at the same point must be necessarily zero as well. Therefore, for the Laughlin and the MR states the three-body recombination rate [43] should be zero, rendering them very stable. However, the MR state is only a good approximation to the true ground state of a boson system interacting with two-body potentials, which implies that in the actual system the recombination rate should be small but not zero.

However, the existence of a Hamiltonian for which the MR state has zero energy allows to perform a *microscopic* analysis of the surface excitations formally analogous to the one carried out for the Laughlin state. Thus it is found that the symmetric polynomials $s_l = \sum_{i=1}^N z_i^l$ describe, also in this case, low-lying excited states of the Hamiltonian V_3 introduced above: The states obtained multiplying the MR state by s_l have zero interaction energy, and therefore are degenerate with the MR state, but adding the confinement term, vL , this degeneracy is lifted. We can identify the surface modes of the MR state with the polynomials s_l , exactly as it was done for the Laughlin state. But it has been shown by several authors [20, 44] that these excitations do not exhaust the spectrum of boundary modes of the MR state. Besides the chiral phonons, which have bosonic character, fermionic excitations that do not carry charge quantum numbers (i.e. they are described by a Majorana fermion) also exist. Lack of charge quantum numbers means that it is not expected that these excitations will be *directly* created by weakly deforming the confining potential (it can happen that the fermionic neutral and the bosonic charged excitations are somehow coupled, but the form of the interaction seems not to be easy to write [45]). Thus we will focus only on the single branch of “charged” surface phonons. By the same arguments employed with other states of scalar bosons, the phonon energy is given (in the

laboratory frame) by $\omega = \omega_\perp l$. But since the MR state is indeed an approximation, we cannot exclude the possibility that the phonon dispersion will receive corrections for $l > 1$ (for $l = 1$ the energy is fixed by Kohn's theorem, as discussed above). However, this does not affect our conclusion that, for the MR state, the dynamic structure factor should display a single surface phonon peak, whose energy is approximately linear with the angular momentum of the mode. One can repeat the steps that lead to the effective field theory for a droplet of MR liquid, and obtain that the spectral weight of the surface phonon in $S_{LAB}(l, \omega)$ is again proportional to $1/m$ with $m = 1$.

V. VECTOR BOSONS

Let us now take up bosons with internal (i.e. hyperfine) degrees of freedom. We call them vector bosons because we will describe them by a field operator that is a tuple of n -fields,

$$\vec{\Psi}^\dagger(z) = (\Psi_0^\dagger(z), \dots, \Psi_{n-1}^\dagger(z)), \quad (50)$$

and which transforms as a vector under $SU(n)$ transformations. This does not necessarily mean that the Hamiltonian has this symmetry, but we will find that under certain conditions the effective theory describing the surface modes does. One can also regard the internal degree of freedom as a spin or pseudo-spin, depending on the context. Thus an n -component vector boson corresponds to a boson of spin $S = (n - 1)/2$. Again, this does not mean that the Hamiltonian is in general rotationally invariant (see below). Scalar bosons (i.e. $S = 0$) are obtained by letting $n = 1$. For $n = 2$ we obtain spin-1/2 bosons, which can be used to describe a mixture of two hyperfine states of the same isotope (as in the experiment reported in Ref. 48). If the atoms are trapped by purely optical means, one can have in the same trap [50] the three magnetic sublevels (i.e. $m_F = -1, 0, +1$) of an isotope of total spin $F = 1$ [55], and this case will be treated by setting $n = 3$. One also can imagine experiments with atoms of higher S (F). In general, however, the interaction will depend on the hyperfine state of the colliding atoms. Thus for $S = 1/2$, it can take the generic form

$$V_{ij} = [g_0 + g_1(\Delta_x S_i^x S_j^x + \Delta_y S_i^y S_j^y + \Delta_z S_i^z S_j^z)] \delta(\mathbf{r}_i - \mathbf{r}_j), \quad (51)$$

for any two particles i and j . For spin-1 bosons in an optical trap rotational invariance implies that [49]

$$V_{ij} = [g_0 + g_1 \mathbf{S}_i \cdot \mathbf{S}_j] \delta(\mathbf{r}_i - \mathbf{r}_j), \quad (52)$$

Higher spin will involve higher powers of $(\mathbf{S}_i \cdot \mathbf{S}_j)$ [49]. Typically one has $|g_1| \ll g_0$, while the sign of g_1 , which determines the ferromagnetic (i.e. $g_1 < 0$, like in ^{87}Rb) or anti-ferromagnetic (i.e. $g_1 > 0$, like ^{23}Na) character of the spin-interaction, depends on the atom species.

We have seen in previous sections that as the amount of angular momentum deposited in the system is increased, all atoms tend to avoid each other. When the atoms have internal degrees of freedom, a cloud containing an equal number of atoms in each internal state will go to a singlet state with zero interaction energy at sufficiently high angular momentum. This possibility has been recently considered by a number of authors for spin-1 [21, 23] as well as for arbitrary spin bosons [18]. The parton construction can be readily applied to study these states. We will consider that the interaction is dominated by the term proportional to g_0 , but including a weak (as it is the usually the case) spin-dependent scattering term makes no difference. We stress that this is because, as long as the interaction has zero-range, these states have zero interaction energy because particles completely avoid each other independently of their internal state.

To see how the parton construction allows us to describe singlet states, we begin by writing the components of field operator, Eq. (50), as the product of two field operators of the fermionic partons, i.e.

$$\Psi_\alpha^\dagger(z) = \psi_1^\dagger(z) \psi_{2\alpha}^\dagger(z), \quad (53)$$

for $\alpha = 0, \dots, n - 1$. In terms of wave functions this implies that the boson wave function reads

$$\Phi_B(z_1 \alpha_1, \dots, z_N \alpha_N) = \Phi_1(z_1^1, \dots, z_N^1) \Phi^{(n)}(z_1^2 \alpha_1, \dots, z_N^2 \alpha_N) \Big|_{\{z_i^1 = z_i^2\}_{i=1, \dots, N}}, \quad (54)$$

where $\Phi_1 = \prod_{i < j} (z_i^1 - z_j^1)$ denotes the Jastrow factor, which describes the state of type-1 partons, whereas $\Phi^{(n)}$ is a Slater determinant of N type-2 partons in internal states $\alpha_1, \dots, \alpha_N$. In this context we are interested in states where all type-2 partons are in the LLL. The situation differs from the case of scalar bosons because now type-2 partons carry the internal degrees of freedom, and therefore states other than the Laughlin state will appear for which the projection onto the LLL is unnecessary. It is interesting to point out that it is the Jastrow factor that ensures

that the resulting wave function has zero interaction energy, while the kinetic energy is quenched to $N\hbar\omega_\perp$ plus the confinement energy. In other words, the factor Φ_1 makes the wave function vanish whenever *any* two-particles approach each other, independently of their internal quantum state. For the same reason, the probability for three particles to approach each other is zero, which in turn implies that the three-body recombination rate vanishes: These states should be particularly long-lived.

To make things more concrete, we specialize our discussion to $n = 2$ components, i.e. $S = \frac{1}{2}$ bosons. We consider this case first because it is simpler but already illustrates the important points, and also because it is relevant to the situation where only two hyperfine states are allowed in the same trap [48]. We will discuss the generalization to arbitrary n at the end of this section. Setting $n = 2$, we assume that $\alpha = 0$ corresponds to spin up (\uparrow) and $\alpha = 1$ to spin down (\downarrow). As mentioned previously, we shall consider only singlet ground states. Therefore, the number of particles, N , must be divisible by $n = 2$, i.e. $N_\uparrow = N_\downarrow = N/2$. Nevertheless, the latter condition does not suffice for Φ_B to be a singlet but only ensures that $S_z|\Phi_B\rangle = 0$. In addition it is needed that

$$S^-|\Phi_B\rangle = 0, \quad (55)$$

where $S^- = \sum_{j=1}^N S_j^- = \sum_{j=1}^N (S_x - iS_y)$ is the operator that decreases the total spin. As the spin index is carried by type-2 partons, the above condition must be indeed met by the parton wave function $\Phi^{(2)}$. Upon filling the LLL with $N/2$ fermions of both spin species, the parton wave function takes the form

$$|\Phi^{(2)}\rangle = \prod_{l=0}^{N/2-1} \psi_{2\uparrow}^\dagger(l) \psi_{2\downarrow}^\dagger(l) |0\rangle, \quad (56)$$

where $|0\rangle$ is the zero particle state. It is not hard to see that this state obeys the condition (55) since the operator $S^- = \sum_{l=0}^{+\infty} \psi_{2\downarrow}^\dagger(l) \psi_{2\uparrow}(l)$ annihilates it. However, in order to obtain the boson wave function, we need the spatial dependence of (56). This is just the product of two Slater determinants of $N/2$ fermions in the LLL, one for each spin orientation, which have the form of the Jastrow wave functions that we have been using throughout. Hence, using Eq. (54), one finds

$$\Phi_{221}(z_1, \dots, z_{N/2}; w_1, \dots, w_{N/2}) = \prod_{i < j=1}^{N/2} (z_i - z_j)^2 (w_i - w_j)^2 \prod_{i,j=1}^{N/2} (z_i - w_j), \quad (57)$$

where z_i and w_i ($i = 1, \dots, N/2$) denote the positions of the spin up and down bosons, respectively. Notice that this wave function seems to have a rather peculiar dependence on z_i and w_i , which is not fully symmetric in these variables, in spite of being a bosonic wave function. However, one must be careful since we are dealing with spinful bosons. Indeed, the above form is what the singlet condition requires. As the reader can easily check for two bosons making a singlet, the anti-symmetry of the spin part of the wave function requires an anti-symmetric spatial wave function. The appropriate generalization of this observation to many particles is given by (57). The Φ_{221} wave function is indeed one of the class introduced by Halperin [15, 47] to describe non-fully spin-polarized quantum Hall states. In Ref. 23 this state was characterized by the *affine* algebra $su(3)_1$, i.e the symmetry of the two-dimensional (conformal) field theory for which the wave function can be obtained as a correlation function (see the appendix for a simple example, and below).

After explaining how to construct some of the vector boson states from partons, we proceed with the description of their surface modes. Indeed, all we need to do is to re-interpret what was done in the previous section for the $n = p = 2$ state. Now j_0 must be interpreted as the charge current, which we denote as j_c in what follows, whereas $j_1/2$ measures the density of the third component of the spin at the boundary, and we denote it as j_s^3 . Therefore,

$$j_c(\theta) = \frac{2}{3} \left[\rho_0(\theta) + \frac{1}{2} (\rho_\uparrow + \rho_\downarrow)(\theta) \right], \quad (58)$$

$$j_s^3(\theta) = \frac{1}{2} (\rho_\uparrow - \rho_\downarrow)(\theta) = \frac{1}{2} \left[\psi_{2\uparrow}^\dagger(\theta) \psi_{2\uparrow}(\theta) - \psi_{2\downarrow}^\dagger(\theta) \psi_{2\downarrow}(\theta) \right]. \quad (59)$$

A difference with respect to the case of scalar bosons is that, in this case, j_c and j_s^3 are decoupled, as long as the trapping potential is spin-independent. The symmetry of the problem is $U(1) \times SU(2)$, where $U(1)$ is associated with the total particle number (i.e. the charge), and therefore with j_c , whereas $SU(2)$ is related to the internal degree of freedom, and therefore to the spin current, j_s^3 . Indeed, the spin current is part of the generators of a larger algebra, which also includes the currents

$$j_s^1 = \frac{1}{2} \left[\psi_{2\uparrow}^\dagger \psi_{2\downarrow} + \psi_{2\downarrow}^\dagger \psi_{2\uparrow} \right], \quad (60)$$

$$j_s^2 = \frac{1}{2i} \left[\psi_{2\uparrow}^\dagger \psi_{2\downarrow} - \psi_{2\downarrow}^\dagger \psi_{2\uparrow} \right]. \quad (61)$$

These three currents can be expressed in a more compact way as $j_s^a(\theta) = \frac{1}{2} \sum_{\alpha,\beta} \psi_\alpha^\dagger(\theta) \sigma_{\alpha\beta}^a \psi_\beta(\theta)$, and they obey the following algebra ($a, b, c = 1, 2, 3$):

$$[j_s^a(l), j_s^b(l')] = \frac{l'}{2} \delta^{ab} \delta_{l+l',0} + i \epsilon_c^{ab} j_c^c(l+l'), \quad (62)$$

known as $su(2)_1$ Kac-Moody algebra.

If decoupled, the charge, j_c , and spin, j_s^3 , currents describe waves that propagate with the same frequency ν . This can be shown using the wave function approach introduced in Sect. III. In this case, each spin orientation is related to different set of symmetric polynomials, $t_l = \sum_{i=1}^{N/2} z_i^l$, $u_l = \sum_{i=1}^{N/2} w_i^l$, with the same excitation energy, $\hbar \nu l$. The charge modes corresponding to the combination $t_l + u_l$ and the spin modes to $t_l - u_l$, are degenerate. Thus we conclude that the dynamics of these modes is dictated by the confining potential (which we have assumed spin-independent). Just like for the Laughlin state, this is a consequence of the wave function Φ_{221} being an exact eigenstate of the Hamiltonian with zero interaction energy. As far as the observable consequences are concerned, it is now possible to consider two dynamic structure factors, given by the correlation functions $\langle j_c(\theta, t) j_c(0) \rangle$ and $\langle j_s^3(\theta, t) j_s^3(0) \rangle$, and related to deformation potentials that couple to the total density, j_c , or the spin density, j_s^3 . In both cases, the observable spectrum will exhibit a single peak at $\omega = \omega_\perp l$. The difference will be in the spectral weight of the peaks, which for the charge peak will be proportional to $\nu = 2/3$, whereas the spin peak to $1/2$. We finally point out that if the confining potential is spin-dependent, then the separation into a charge and a spin density current is no longer convenient. In other words, the currents j_c and j_s^2 do not correspond to the normal modes of the system any more. In such a case, for instance, the spectrum for a trapping potential deformation that couples to the total charge will display two peaks at two different frequencies $\omega = \omega_{\uparrow\perp} l$ and $\omega = \omega_{\downarrow\perp} l$ (we assume that $\omega_{\uparrow,\downarrow\perp} - \Omega \ll \Omega$). The total spectral weight of the two peaks, however, will be again proportional to $2/3$, each peak contributing $1/3$.

As a final demonstration of the internal consistency of these constructions, we will rederive the wave function Φ_{221} using the formalism explained in the appendix, and which relates the wave function to the correlation functions of the effective theory for surface modes. The key to this approach is to identify the boson operator in the LLL with the vertex operator (see appendix for a definition) that describes the boson operator at the boundary. To this purpose, let us introduce the phonon fields for the partons, in analogy to how it was defined in Sect. III, i.e.

$$\partial_\theta \phi_0(\theta) = 2\pi \rho_0(\theta), \quad (63)$$

$$\partial_\theta \phi_\alpha(\theta) = 2\pi \rho_\alpha(\theta), \quad (64)$$

with $\alpha = \uparrow, \downarrow$. The the parton construction dictates that the boson field operator at the boundary takes the form [19]

$$\Psi_\alpha^\dagger(\theta) = e^{-i(\phi_0 + \phi_\alpha)(\theta)}, \quad (65)$$

which is nothing but Eq. (53) with the parton fields written as exponentials of their corresponding phonon fields (cf. Sect. III). However, the phonon fields $\phi_0, \phi_\uparrow, \phi_\downarrow$, just as the currents $\rho_0, \rho_\uparrow, \rho_\downarrow$, are not independent. Only j_c and j_s^3 are independent. But the following expressions:

$$\rho_0 + \rho_\uparrow = \frac{3}{2} j_c + j_s^3, \quad (66)$$

$$\rho_0 + \rho_\downarrow = \frac{3}{2} j_c - j_s^3, \quad (67)$$

help us to relate the phonon field combinations that enter in Ψ_α^\dagger to the charge and spin phonon fields, defined by the following equations:

$$\partial_\theta \varphi_c(\theta) = 2\pi \sqrt{\frac{3}{2}} j_c(\theta), \quad (68)$$

$$\partial_\theta \varphi_s(\theta) = 2\pi \sqrt{2} j_s^3(\theta). \quad (69)$$

These fields have been so normalized that their vertex operators have the two-point correlation functions:

$$\langle V_{+1}^i(\bar{z}) V_{-1}^j(0) \rangle = \langle : e^{i\varphi_i(\bar{z})} : : e^{-i\varphi_j(0)} : \rangle = \frac{\delta_{ij}}{z}, \quad (70)$$

where $i, j = c, s$. The field operators read

$$\Psi_{B\uparrow}^\dagger(\bar{z}) = : e^{-i(\sqrt{\frac{3}{2}}\varphi_c + \frac{1}{\sqrt{2}}\varphi_s)(\bar{z})} : , \quad (71)$$

$$\Psi_{B\downarrow}^\dagger(\bar{z}) = : e^{-i(\sqrt{\frac{3}{2}}\varphi_c - \frac{1}{\sqrt{2}}\varphi_s)(\bar{z})} : . \quad (72)$$

We are now ready to compute the wave function. It takes the form

$$\begin{aligned}
\Phi_{221}(\bar{z}_1, \dots, \bar{z}_{N/2}; \bar{w}_1, \dots, \bar{w}_{N/2}) &= \left\langle \prod_{i=1}^{N/2} \Psi_{\uparrow}^{\dagger}(\bar{z}_i) \Psi_{\uparrow}^{\dagger}(\bar{w}_i) : e^{i\sqrt{\frac{3}{2}} \int_{|z|<R} d^2z \varphi_c(\bar{z}) \rho_o} : \right\rangle \\
&= \left\langle \prod_{i=1}^{N/2} V_{-\sqrt{\frac{1}{2}}}^s(\bar{z}_i) V_{+\sqrt{\frac{1}{2}}}^s(\bar{w}_i) \right\rangle \left\langle \prod_{i=1}^{N/2} V_{-\sqrt{\frac{1}{2}}}^c(\bar{z}_i) V_{-\sqrt{\frac{1}{2}}}^c(\bar{w}_i) : e^{i\sqrt{\frac{3}{2}} \int_{|z|<R} d^2z \varphi_c(\bar{z}) \rho_o} : \right\rangle \\
&= \prod_{i<j=1}^{N/2} (\bar{z}_i - \bar{z}_j)^{1/2} (\bar{w}_i - \bar{w}_j)^{1/2} \prod_{i,j=1}^{N/2} (\bar{z}_i - \bar{w}_j)^{-1/2} \\
&\quad \times \prod_{i<j=1}^{N/2} (\bar{z}_i - \bar{z}_j)^{3/2} (\bar{w}_i - \bar{w}_j)^{3/2} \prod_{i,j=1}^{N/2} (\bar{z}_i - \bar{w}_j)^{3/2} \prod_{i=1}^{N/2} e^{-(|z_i|^2 + |w_i|^2)/2\ell^2} \\
&= \prod_{i<j=1}^{N/2} (\bar{z}_i - \bar{z}_j)^2 (\bar{w}_i - \bar{w}_j)^2 \prod_{i,j=1}^{N/2} (\bar{z}_i - \bar{w}_j) \prod_{i=1}^{N/2} e^{-(|z_i|^2 + |w_i|^2)/2\ell^2}. \tag{73}
\end{aligned}$$

This is just the anti-analytic version of the Halperin 221 state, Eq. (57). In the above expressions R is the radius of the disk of positive charge background with density $\rho_o = \nu/\pi\ell^2 = 2/(3\pi\ell^2)$ and total charge equal to N . It is also interesting to notice that, in the above construction the wave function splits into two factors, one involving only charge (φ_c) and other involving only spin (φ_s) operators. This decomposition can be understood as due to the separation of the fundamental boson into two kinds of excitations: a *spinon*, which carries the spin, and a *holon*, which carries the “charge”.

Finally, the generalization to arbitrary n is not hard to work out. For a number of particles divisible by n , the singlet $SU(n)$ wave function reads:

$$\Phi\left(\left\{z_1^\alpha, \dots, z_{N/n}^\alpha\right\}_{\alpha=0, \dots, n-1}\right) = \left[\prod_{\alpha=0}^{n-1} \prod_{i<j=1}^{N/n} (z_i^\alpha - z_j^\alpha)^2\right] \left[\prod_{\alpha<\beta} \prod_{i,j=1}^{N/n} (z_i^\alpha - z_j^\beta)\right], \tag{74}$$

where $\alpha, \beta = 0, \dots, n-1$ (This state is the $su(n+1)_1$ state of Ref. [23]). Just as we did above, one can construct the surface modes from the symmetric polynomials, $s_l^{(\alpha)} = \sum_{i=1}^{N/n} \left(z_i^{(\alpha)}\right)^l$, which will have excitation energy (in the rotating frame) $\hbar v_\alpha l$, with $v_0 = v_1 = \dots = v_{n-1} = v \equiv \omega_\perp - \Omega$ if the trapping potential is spin-independent. The parton construction yields n independent currents, one of them, $j_c = (n\rho_0 + \sum_{i=1}^{n-1} \rho_i)/(n+1)$, corresponding to the total current and is therefore associated with the charge $U(1)$ symmetry. The remaining $n-1$ currents are part of a $su(n)_1$ algebra that describes the dynamics of the internal degree of freedom. The dynamic structure factor related to the $\langle j_c(\theta, t) j_c(0) \rangle$ correlator exhibits a single peak at $\omega = \omega_\perp l$, whose intensity is proportional to $\nu = n/(n+1)$. If the trapping potential is spin-dependent, however, this peak splits into as many peaks as distinct values of the frequency $\omega_{\alpha\perp}$ exist, but the total intensity remains proportional to $n/(n+1)$ each spin component contributing $1/(n+1)$.

VI. CONCLUSIONS AND OUTLOOK

In this paper we have described the surface modes of ultra-cold atomic clouds with a very large number of vortices. These systems are known as vortex liquids, and are expected to be observed in the critical rotation regime where the rotation frequency approaches the trap frequency. The surface waves of vortex liquids present several important differences with respect to the surface modes of a Bose condensate. For an axially symmetric trap of the type considered above, the frequency dispersion of the surface modes of a BEC is found to be [49]:

$$\omega = \omega_\perp \sqrt{|l|}, \tag{75}$$

where $l = 0, \pm 1, \pm 2, \dots$. On the other hand, for a spin-independent trap, a vortex liquid exhibits surface modes whose dispersion is well approximated by

$$\omega = \omega_\perp l, \tag{76}$$

where $l = 1, 2, 3, \dots$ i.e. a positive integer, which measures by how many quanta is increased the total angular momentum of the vortex liquid. We also found other (approximate) excitations, which involve promoting particles to

higher Landau levels, and which have the same energy as the surface modes in the laboratory frame. However, these excitations decrease the total angular momentum by $l = 1, 2, \dots$ quanta. However, we must stress that the surface modes are the true low-lying excitations of the vortex liquids as they dominate their low-temperature properties (for $T \ll \hbar\Omega$) since it is their energy in the rotating frame, not that in the laboratory frame, that enters the Boltzmann factor. Furthermore, we argue that for $T \gg \hbar(\omega_\perp - \Omega)$, their intensity in the dynamic structure factor should be much larger.

The chirality of the surface modes, namely that l is restricted to positive integers, is a consequence of the dramatic effect that rapid rotation has on a cloud of ultra-cold atoms: Besides enhancing quantum fluctuations, which are finally responsible for the destruction of the condensate and the melting of the Abrikosov lattice, fast rotation, when regarded from the rotating reference frame, has the same effect as a strong magnetic field on a system of charged particles moving in two dimensions. In both situations, time-reversal symmetry is broken, which leads to the chirality of surface modes. We find, by comparing with the angular momentum and excitation energy of bulk excitations of the Laughlin liquid, that the surface waves are the low-lying modes of the system. Indeed, quasi-holes and quasi-particles are bulk excitations that change the total angular momentum by $\sim \hbar N$, whereas the surface modes do it just by $l \lesssim \sqrt{mN}$ quanta. We expect that this property also holds for the more complicated vortex liquids described in Sect. IV. For these states, we find that there exist more than one branch of surface phonons. This result is obtained by relying on the composite-fermion ansatz used in Ref. 10 and first introduced for fermions in Ref. 28. In this picture, a bound state of a boson with a vortex is an object of fermionic statistics, known as composite fermion, which occupies n “renormalized” Landau levels. The parton construction [19] used in our calculations in a concrete implementation to study surface excitations of the composite-fermion idea.

We propose to probe the surface excitations by adding a weak time-dependent part to the trapping potential that imparts small amounts of angular momentum to the system. This should excite surface waves in droplets of vortex liquid. We have quantified the response of the system in terms of the dynamic structure factor $S_{LAB}(l, \omega)$. This function is related to the density correlation-function at the boundary. If the residual interactions between the composite fermions can be neglected, $S_{LAB}(l, \omega)$ should exhibit a single peak at the frequency given by Eq. (76). However, in the case where residual interactions are not negligible, several peaks may appear for $l > 1$. We also find that the spectral weight of the surface modes in $S_{LAB}(l, \omega)$, is proportional to $p/(p+1)$, where p is a positive integer. This means that if the system is gradually driven to states of higher angular momentum, going through different vortex liquids at every stage, the integer p characterizing the peak intensity of the surface modes, should decrease down to $p = 1$, which corresponds to the system being in Laughlin state with $\nu = \frac{1}{2}$ (higher angular momentum states can be imagined but this would be experimentally much harder). In other words, the total intensity in $S_{LAB}(l, \omega)$ of the surface modes at a given l should decrease as the Laughlin $\frac{1}{2}$ state is approached, at constant temperature.

Finally, we have also found chiral surface waves in vortex liquids of vector (i.e. spinful) bosons. In this case, the parton construction, used to study the surface waves of scalar bosons, can be also successfully applied. If the trapping potential is spin independent, the experimental signatures are similar to those for states of scalar bosons with p equal to the number of components of the boson field (2 for spin $\frac{1}{2}$ bosons, 3 for $S = 1, \dots, 2S + 1$ spin- S bosons). However, in this case the surface-phonon peak is always to be found for $\omega = \omega_\perp l$, where $l > 0$. In spin-dependent traps, as long as the difference $v_\alpha = \omega_{\alpha\perp} - \Omega \ll \Omega$ ($\alpha = 1, \dots, 2S + 1$), the peak splits into as many peaks as distinct values of $\omega_{\alpha\perp}$ exist.

The study of the surface modes has also produced other results. We have found that the peak intensity of the surface phonon in the Laughlin liquid is proportional to $1/m$, where m is the inverse of the filling fraction. This was interpreted as if the bosons in the Laughlin liquid behave as “super-fermions” which, on average, occupy two states per particle. This is a particular example of the generalized exclusion statistics first discussed by Haldane [24]. This feature of the spectral weight of the surface modes of the Laughlin state can be interpreted as an experimental manifestation of this exotic exclusion statistics. In addition, by analyzing the behavior of one-body density matrix near the boundary, we are able to obtain the occupancy of the orbitals with the highest angular momentum in the Laughlin state. For $m > 1$, we have argued that the behavior of the occupancy near the boundary forces a maximum in the occupancy before it decays to zero at $l = l_{max} = m(N - 1)$, where N is the number of particles in the droplet. This maximum has its correspondence in the density profile, which should be a hallmark of the Laughlin liquid, and possibly of other vortex liquids as well. Last but not least, we have argued that the Laughlin liquid and the singlet states of vector bosons, should be very stable with respect to three-body losses. This is because their wave functions vanish when any two particles approach each other. The Moore-Read state that provides a good approximation to the state of total angular momentum $L \approx N^2/2$ for scalar bosons, should also be very stable since its wave function vanishes when any three particles come to the same point. However, since this state is only a good approximation to the actual ground state, we expect it to be less stable than the Laughlin state, which is exact.

In spite of the successes of the constructions presented in this work, there remain a number of important open problems. An important one is related to the accuracy of the description given here to describe the surface modes of vortex liquids of scalar bosons. The description seems to be well established for the Laughlin state, but for the other

stable states found at lower angular momentum it should be checked numerically. This can be done by analyzing the low-lying excitations of the states found in Ref. 10. We expect that the analysis performed here will encourage further studies in this direction, which may prove or disprove the conclusions of our analytical work. Another interesting issue that has not been addressed in this article is the possibility that not all the excitations predicted by the parton construction are indeed surface modes. This problem was numerically analyzed for fermion systems in Ref. 36, where it was argued that the effective theory for the surface waves of states in the (fermionic) Jain sequence is a $\mathcal{W}_{1+\infty}$ minimal model instead of the larger (in the sense that it has larger spectral degeneracies, but the same spectrum) $u(1) \times su(n)_1$ model, which results from the parton construction used in the present work (see Ref. 36 and references therein). Similar comments apply to the other states of vector bosons which have not been considered in this paper, but which were recently constructed in Ref. [23]. To sum up, we can say that we have just begun to scratch the surface of the rich phenomena offered by this new setup for strong correlation and quantum Hall physics.

Acknowledgments

The author wants to express his gratitude to Erich Mueller for a useful suggestion. He also gratefully acknowledges useful correspondence with Nicola Wilkin and helpful conversations with Ignacio Cirac, Marina Huerta, Alexander Nersesyan, Antonio Sarsa, Subodh Shenoy, and Peter Zoller. Financial support provided by the ESF programme “BEC 2000+” for a visit to the MPQ in Garching (Germany) is gratefully acknowledged.

APPENDIX A: RELATIONSHIP BETWEEN PROPERTIES IN THE LABORATORY AND ROTATING FRAMES. THE DIPOLE MODE AND GENERALIZED KOHN’S THEOREM

In BEC’s of ultra-cold dilute gases time-of-flight and *in situ* imaging of shape oscillations, as well as Bragg scattering [32, 50], have been used to measure the excitation spectrum. Light scattering in general, and Bragg scattering in particular, allow to access the dynamic structure factor $S(\mathbf{q}, \omega)$ [32, 50]. Whatever the method of choice, here we shall imagine a situation where a time-dependent non axi-symmetric potential is added to the trapping potential in such a way that it drives the system slightly out of equilibrium by exciting surface modes. The response to the potential is measured and since we are interested in the *linear response* regime, we shall assume throughout that the perturbation is weak. All the measurements are performed in the laboratory (or LAB, for short) reference frame. At this point it is convenient to recall the steps needed in the preparation of a rotating cloud. One of the commonly used methods consists in adding a time-dependent and non-cylindrically symmetric part, pretty much like the perturbation that we shall consider later, which imparts angular momentum to a conveniently cooled BEC. We shall assume that the cloud has been subjected to this “stirring potential” for some time, driven at some angular frequency Ω_d . When enough angular momentum has been deposited in the system, the external force is turned off and the cloud reverts to a cylindrically symmetric situation, where the Hamiltonian has the form discussed in Sect. II. Under these conditions, for an axially symmetric trap, the angular momentum along the axis, L , is a conserved quantity (i.e. it commutes with the Hamiltonian). This means that the total angular momentum imparted to the system will remain constant subsequently, rotating at a frequency $\Omega \neq \Omega_d$ [13]. Next we imagine that in this situation the system is perturbed again by switching on a weak time-dependent stirring force. In the LAB frame, this perturbation is described by adding to the Hamiltonian the following term:

$$U_{LAB}(t) = \int d\mathbf{r} \delta v_{LAB}(\mathbf{r}, t) \rho(\mathbf{r}). \quad (\text{A1})$$

In the previous expression, we have neglected any dependence on the axial coordinate. Furthermore, in order to excite predominantly surface modes, a multipole expansion of the external potential $\delta v_{LAB}(r, \theta, t)$ should not contain high multipole terms. This means that it will be a smooth function of r near the boundary of the boson droplet, i.e. for $r \approx R$. If we further assume that the external potential contains no monopole mode, i.e.

$$\int_0^{2\pi} d\theta \delta v_{LAB}(r, \theta, t) = 0, \quad (\text{A2})$$

then we can write

$$U_{LAB}(t) = \int d\mathbf{r} \delta v_{LAB}(\mathbf{r}, t) [\rho(\mathbf{r}) - \rho_o(r)] \approx \int_0^{2\pi} d\theta \delta v_{LAB}(R, \theta, t) \int_0^{+\infty} dr r [\rho(r, \theta) - \rho_o(r)], \quad (\text{A3})$$

where the last expression follows from the smoothness of the potential near the boundary of the droplet. The expression integrated over r is the boundary density operator, $j(\theta)$. Hence

$$U_{LAB}(t) = \int_0^{2\pi} d\theta \delta v_{LAB}(R, \theta, t) j(\theta). \quad (\text{A4})$$

This corresponds to the perturbation discussed in the main text, but expressed in the LAB frame. The ROT and LAB are related by the unitary transformation

$$\mathcal{U}(t) = e^{iL\Omega t/\hbar}. \quad (\text{A5})$$

Notice that this transformation will affect only those correlation functions which are time-dependent (e.g. like the dynamic structure factor). Time-independent correlation functions, such like the one-body density matrix and its diagonal part, the equilibrium density profile, are unchanged when going from one reference frame to the other. To see how the dynamic structure factor computed in the rotating (ROT, for short) frame is related to measurements in the LAB frame, which is where the measurement apparatus is actually placed, we need to work out the effects of the perturbation, Eq. (A4), in LAB. Starting from the time-dependent Schrödinger equation,

$$i\hbar\partial_t|\Phi_{LAB}(t)\rangle = [H_{LAB} + U_{LAB}(t)]|\Phi_{LAB}(t)\rangle. \quad (\text{A6})$$

we find that, to linear order in $U_{LAB}(t)$, the wave function is modified to

$$|\Phi_{LAB}^I(t)\rangle \approx |\Phi_{LAB}^I(-\frac{T_o}{2})\rangle - \frac{i}{\hbar} \int_{-\frac{T_o}{2}}^t dt' U_{LAB}^I(t') |\Phi_{LAB}^I(t')\rangle, \quad (\text{A7})$$

where the interaction representation has been used:

$$|\Phi^I(t)\rangle = e^{iH_{LAB}t/\hbar}|\Phi(t)\rangle, \quad (\text{A8})$$

$$U^I(t) = e^{iH_{LAB}t/\hbar}U(t)e^{-iH_{LAB}t/\hbar}. \quad (\text{A9})$$

Before going any further, it is convenient to recall that the Hamiltonians in the ROT and LAB frames are related by the following expression

$$H_{ROT} = H_{LAB} - \Omega L, \quad (\text{A10})$$

where $[L, H_{LAB}] = 0$, as the trap potential is cylindrically symmetric (this is not so after $U_{LAB}(t)$ is turned on). This expression is obtained by transforming the time-dependent Schrödinger equation, (A6) to the ROT frame using Eq. (A5). Indeed, it is the quantum analog of the classical relationship $E_{ROT} = E_{LAB} - \Omega L$.

Assuming that, in the ROT frame, at time $t = -\frac{T_o}{2}$ the system is in a state $|\Phi_n\rangle$ with probability given by the Boltzmann weight $e^{-E_n^{ROT}/T}$, we compute the probability per unit time for large T_o that the system is found, also in the ROT frame, in a state $|\Phi_m\rangle$ at $t = T_o/2$ (we choose $H_{ROT}|\Phi_\alpha\rangle = E_\alpha^{ROT}|\Phi_\alpha\rangle$ and $L|\Phi_\alpha\rangle = L_\alpha|\Phi_\alpha\rangle$, $\alpha = n, m$. The calculation, however, is performed in the LAB frame). The result can be written as

$$\Gamma(T, \Omega) = \frac{1}{2\pi} \sum_{l=-\infty}^{+\infty} \int_{-\infty}^{+\infty} \frac{d\omega}{2\pi} |\delta v_{LAB}(R, l, \omega)|^2 S_{ROT}(l, \omega - l\Omega). \quad (\text{A11})$$

Therefore, we can define the dynamic structure factor in the LAB frame as

$$S_{LAB}(l, \omega) = S_{ROT}(l, \omega - l\Omega). \quad (\text{A12})$$

where the dynamic structure factor,

$$S_{ROT}(l, \omega) = \int_{-\infty}^{+\infty} dt \int_0^{2\pi} d\theta' e^{i\omega t - il\theta'} \langle j(\theta', t) j(0) \rangle = \frac{2\pi\hbar}{Z} \sum_{\alpha, \beta} e^{-E_\alpha^{ROT}/T} |\langle \beta | j(l) | \alpha \rangle|^2 \delta(\hbar\omega + E_\alpha^{ROT} - E_\beta^{ROT}). \quad (\text{A13})$$

There is a simple explanation for the transformation law, Eq. (A12). The shift $\omega \rightarrow \omega - l\Omega$ is precisely the frequency in the ROT frame of an excitation of angular momentum $\hbar l$ and energy $\hbar\omega$ in the LAB frame. The other component in the dynamic structure factor are the oscillator strengths $|\langle \alpha | j(l) | \beta \rangle|^2$ for transitions induced between different eigenstates of H_{ROT} (and also of H_{LAB} , since it commutes with L). Since the ROT and LAB frames are related by a unitary

transformation, which leaves these probabilities unchanged, only the delta function in ω is affected by the change of reference frame.

Eq. (A11) implies that we can measure $S_{LAB}(l, \omega)$ by cleverly choosing the external perturbation δv_{LAB} . It is important to point out that in the discussion in the main text, we have omitted any reference to the dependence of the intensity of the response on the droplet radius, R , coming from $\delta v_{LAB}(R, l, \omega)$. When analyzing the experimental data this fact must be taken into account since R , defined as the semiclassical radius of the droplet, depends on the effective filling fraction ν . For instance, for a Laughlin droplet we found that $R = \sqrt{mN} \ell$, and in general $R = \sqrt{N/\nu} \ell$, being the *average* density given by $\nu/\pi\ell^2$. Thus, besides the factor $\nu = p/(p+1)$, with p a non-negative integer, discussed in previous sections, the strength of the peak in response to an l -polar potential $\delta v_{LAB} \sim e^{il\theta}$ is also proportional to R^l . This factor is especially important when analyzing the dipole mode (i.e. $l = 1$). This is because the energy and the peak intensity of this mode are given, for a many-body system confined in a harmonic trap, by the generalized Kohn's theorem [51, 52]. This theorem follows from the fact in a harmonic trap the motion of the center of mass decouples from other motions of the system. Introducing the operators:

$$\mathbf{\Pi} = \sum_{j=1}^N [\mathbf{p}_j - M\Omega \hat{\mathbf{z}} \times \mathbf{r}_j], \quad (\text{A14})$$

$$\mathbf{R} = \frac{1}{N} \sum_{j=1}^N \mathbf{r}_j, \quad (\text{A15})$$

the Hamiltonian (in the ROT frame) splits into two commuting parts (cf. Eq. (2)),

$$H_{ROT} = H_{CM} + H_R, \quad (\text{A16})$$

$$H_{CM} = \frac{\mathbf{\Pi}^2}{2MN} + \frac{MN}{2}(\omega_{\perp}^2 - \Omega^2)\mathbf{R}^2. \quad (\text{A17})$$

To study the excitation of the center-of-mass degrees of freedom it is convenient to use the set *independent* operators,

$$A^{\dagger} = \frac{\Pi_x + i\Pi_y}{M} - i(\omega_{\perp} + \Omega)N(X + iY), \quad (\text{A18})$$

$$B^{\dagger} = \frac{\Pi_x - i\Pi_y}{M} + i(\omega_{\perp} - \Omega)N(X - iY), \quad (\text{A19})$$

which have the following properties:

$$[H_{ROT}, A^{\dagger}] = \hbar\omega_A A^{\dagger}, \quad (\text{A20})$$

$$[H_{ROT}, B^{\dagger}] = \hbar\omega_B B^{\dagger}, \quad (\text{A21})$$

$$[L, A^{\dagger}] = \hbar A^{\dagger}, \quad (\text{A22})$$

$$[L, B^{\dagger}] = -\hbar B^{\dagger}, \quad (\text{A23})$$

where $\omega_A = \omega_{\perp} - \Omega$, i.e. the energy of $l = 1$ surface mode, which in the LAB frame will have an energy equal to $\hbar\omega_{\perp}$. The theorem also predicts the existence of another Kohn mode, at $\omega_B = \omega_{\perp} + \Omega$ in the ROT frame. Notice that although this mode has much higher energy in the ROT frame, it actually reduces the angular momentum by one quantum and therefore, application of the formula $E_{ROT} = E_{LAB} - \Omega L$, yields an excitation energy in the LAB frame equal to ω_{\perp} . Thus we conclude that the center-of-mass modes created by acting with the operators A^{\dagger} and B^{\dagger} on the many-body ground state are *degenerate* in the LAB frame. However, since the system is in thermal equilibrium in the ROT frame, it is the energy in this system that enters in the Boltzmann factor, $e^{-E_n^{ROT}/T}$. Hence, at temperatures $T \ll \hbar\Omega$, the probability of finding the system in the state $A^{\dagger}|0\rangle$ is overwhelmingly larger than the probability of finding it in $B^{\dagger}|0\rangle$. By their quantum numbers we can identify $A^{\dagger} \sim s_1 = \sum_{j=1}^N z_j$, and $B^{\dagger} \sim d_1 \sim \sum_{j=1}^N \bar{\pi}_j \sim \sum_{j=1}^N \bar{z}_j$, and as we argued in Sect. III, the former yields a low-lying state whereas the latter does not.

Let us finally compute the the peak intensity of the mode created by A^{\dagger} :

$$f(l=1, T=0) = |\langle 1|N(X + iY)|0\rangle|^2 = \frac{1}{4\omega_{\perp}^2} |\langle 1|(A^{\dagger} - B)|0\rangle|^2, \quad (\text{A24})$$

where $|1\rangle = A^{\dagger}|0\rangle/\sqrt{[A, A^{\dagger}]}$. Thus we obtain

$$f(l=1, T=0) = \frac{\hbar N}{M\omega_{\perp}} = N\ell^2. \quad (\text{A25})$$

This is in agreement with the predictions of effective field theory once the dependence on R has been taken into account. For instance, consider a Laughlin droplet perturbed by the dipolar potential $N(X + iY)e^{-i\omega t}$, i.e. $\delta v_{LAB}(R, \theta, t) \sim R e^{i\theta} e^{-i\omega t}$. Using Eq. (A11) and the results of Sect. III

$$f(l = 1, T = 0) = R^2 \frac{1}{m} = N\ell^2 \quad (\text{A26})$$

where we have used $R = \sqrt{mN}\ell$. This result is identical to the one obtained by the generalized Kohn's theorem, as it should be. For states with several branches of surface phonons $R^2 = N\ell^2/\nu$, and since the total spectral weight of $S_{LAB}(l, \omega)$ for $l = 1$ equals $\nu = p/(p + 1)$ (p integer), and taking into account that $R^2\nu = N\ell^2$, we see that all the spectral weight must be concentrated in a single peak at $\omega = \omega_\perp$. Therefore, all corrections to the energy of the surface modes must vanish for $l = 1$, as discussed in Sect. IV, making all branches degenerate at this particular angular momentum.

APPENDIX B: PLASMA FORMALISM AND VERTEX OPERATORS

In this appendix we shall introduce the plasma formalism, which is a convenient tool to study some properties of quantum Hall wave functions. However, our main goal here is to establish a deep connection between this formalism and the correlation functions of a two-dimensional gaussian field theory [20, 53]. As we show below for the Laughlin state, the N -particle wave function can be obtained as the multipoint correlation function of N objects, known as vertex operators, plus another operator, which yields the gaussians omitted so far. The vertex operators are then related to the boundary field operators introduced in Sect. III. The construction shows explicitly the relationship between the low-energy description of surface modes, and the bulk wave functions. The results of this section are used in Sect. V for the slightly more complicated case of vector bosons. Finally, we also show how to obtain the one-body density matrix, Eq. (26).

Consider the wave function for Laughlin state

$$\Phi_m(z_1, \dots, z_N) = \mathcal{N} \prod_{i < j=1}^N (z_i - z_j)^m \prod_{i=1}^N e^{-|z_i|^2/2\ell^2}. \quad (\text{B1})$$

The (unnormalized) probability density can be written as

$$P_m(\mathbf{r}_1, \dots, \mathbf{r}_N) = |\Phi_m(z_1, \dots, z_N)|^2 = \exp[-\beta U(\mathbf{r}_1, \dots, \mathbf{r}_N)], \quad (\text{B2})$$

where $\beta = 2m$ and

$$U(\mathbf{r}_1, \dots, \mathbf{r}_N) = \frac{1}{2m\ell^2} \sum_{i=1}^N |z_i|^2 - \sum_{i < j=1}^N \log |z_i - z_j|, \quad (\text{B3})$$

is the potential energy of a one-component classical plasma in two dimensions. The plasma consists of N identical particles with unit charge moving on a uniform neutralizing background of charge density $\rho_o = 1/m\pi\ell^2$. The plasma is neutral if the background takes up a disk of radius $R = \sqrt{(\pi\rho_o)^{-1}N} = \sqrt{mN}\ell$. To understand the analogy, let us recall that in two dimensions the Coulomb potential due to a unit charge reads

$$g(\mathbf{r} - \mathbf{r}') = -\log |\mathbf{r} - \mathbf{r}'| + \text{const.} = -\log |z - z'| + \text{const.} \quad (\text{B4})$$

In addition, a uniform background of charge ρ_o creates a potential at \mathbf{r} (with $|\mathbf{r}| < R$) given by

$$g_{BG}(\mathbf{r}) = \int_{|\mathbf{r}'| < R} d\mathbf{r}' g(\mathbf{r} - \mathbf{r}') \rho_o = -\frac{\pi\rho_o}{2} |z|^2, \quad (\text{B5})$$

as can be easily checked using Poisson's equation: $\nabla^2 g_{BG}(\mathbf{r}) = -2\pi\rho_o$. Putting everything together, Eq. (B3) is obtained.

It will be useful to rewrite (B2) as follows

$$P_m[\rho] = \frac{Z_{\text{gauss}}[\rho]}{Z_{\text{gauss}}[0]}, \quad (\text{B6})$$

where $Z_{\text{gauss}}[\rho]$ is the functional integral

$$Z_{\text{gauss}}[\rho] = \int [du(\mathbf{r})] e^{-\beta \int d\mathbf{r} \left[\frac{1}{4\pi} (\nabla u(\mathbf{r}))^2 - i\rho(\mathbf{r})u(\mathbf{r}) \right]}, \quad (\text{B7})$$

where $\rho(\mathbf{r}) = -\sum_{i=1}^N \delta(\mathbf{r} - \mathbf{r}_i) + \rho_o \vartheta(R - |\mathbf{r}|)$ is the total charge density of the plasma ($\vartheta(r)$ is the step function). The above expression can be shown to be equivalent to Eq. (B2) by shifting

$$u(\mathbf{r}) = u'(\mathbf{r}) + i \int d\mathbf{r}' g(\mathbf{r} - \mathbf{r}') \rho(\mathbf{r}'), \quad (\text{B8})$$

which cancels the term linear in $u(\mathbf{r})$ in (B7) and yields the following expression for the potential energy of the plasma

$$U(\mathbf{r}_1, \dots, \mathbf{r}_N) = U[\rho] = \frac{1}{2} \int d\mathbf{r} \rho(\mathbf{r}) g(\mathbf{r} - \mathbf{r}') \rho(\mathbf{r}'). \quad (\text{B9})$$

Substituting $\rho(\mathbf{r})$ defined as above, this expression reduces to (B3) (the charge self-energies can be removed by redefining $g(\mathbf{r}) = -\log[|\mathbf{r}|^2 + \alpha^2]/\alpha^2$ and carefully taking $\alpha \rightarrow 0$ at the end).

We have taken so much work to show that $P(\mathbf{r}_1, \dots, \mathbf{r}_N)$ can be written as the functional integral (B7) because this form allows us to make a very useful connection. Indeed Eq. (B7) is the “generating functional” of a two-dimensional field theory: For arbitrary $\rho(\mathbf{r})$, it generates all correlation functions of a gaussian field theory, which describes, e.g., the classical statistical mechanics of a two-dimensional superfluid or the quantum mechanics in imaginary time of a one-dimensional quantum fluid [54]. If we specialize to $\rho(\mathbf{r}) = \rho_o \vartheta(R - |\mathbf{r}|) - \sum_{i=1}^N \delta(\mathbf{r} - \mathbf{r}_i)$, then Eq. (B7) generates N -point correlation functions of the form

$$P(\mathbf{r}_1, \dots, \mathbf{r}_N) = \langle e^{-2imu(\mathbf{r}_1)} \dots e^{-2imu(\mathbf{r}_N)} e^{+2im \int_{|\mathbf{r}| < R} d\mathbf{r} u(\mathbf{r}) \rho_o} \rangle, \quad (\text{B10})$$

If instead of regarding this correlation function as a statistical average in two dimensions, we think of it as a quantum expectation value in one dimension, the objects $e^{2miu(\mathbf{r})}$ represent operators, termed “vertex” operators. The field operator $u(\mathbf{r})$ obeys the equation of motion $\nabla^2 u(\mathbf{r}) = 0$, i.e. the Laplace equation. This also corresponds to the equation of motion of a phonon field in imaginary time. Recalling that any solution of Laplace’s equation can be written as the linear combination of an analytic and an anti-analytic part, let us write

$$u(\mathbf{r}) = \frac{1}{2\sqrt{m}} [\bar{\varphi}(\bar{z}) - \varphi(z)], \quad (\text{B11})$$

where $z = x + iy$ and $\bar{z} = x - iy$ and the normalization $1/\sqrt{m}$ has been introduced for later convenience. Next, notice that the above field operators obey the (first order) equations of motion:

$$\partial_z \bar{\varphi}(\bar{z}) \equiv \frac{1}{2} (\partial_x - i\partial_y) \bar{\varphi}(x - iy) = 0, \quad (\text{B12})$$

$$\partial_{\bar{z}} \varphi(z) \equiv \frac{1}{2} (\partial_x + i\partial_y) \varphi(x + iy) = 0. \quad (\text{B13})$$

The structure of these equations resembles very much the equation of motion for the *chiral* phonon field $\phi(\theta)$ introduced in Sect. III. Recall that there it was found that $\phi(\theta, t) = \phi(\theta - vt)$, which in imaginary time $\tau = it$ obeys $(v^{-1}\partial_\tau + i\partial_\theta) \phi(v\tau - i\theta) = 0$. In an analogous way as we did for $\phi(\theta)$ in terms of $e^{i\theta}$, we can expand the fields φ and $\bar{\varphi}$ in a series of z and \bar{z} , respectively. These expansions read:

$$\varphi(z) = -\varphi_o - iq \log z + \sum_{l>0} \frac{1}{\sqrt{l}} [z^{-l} c(l) + z^l c^\dagger(l)], \quad (\text{B14})$$

$$\bar{\varphi}(\bar{z}) = \bar{\varphi}_o + i\bar{q} \log \bar{z} + \sum_{l>0} \frac{1}{\sqrt{l}} [z^{-l} \bar{c}(l) + \bar{z}^l \bar{c}^\dagger(l)], \quad (\text{B15})$$

where $[q, \varphi_o] = i$, $[c(l), c^\dagger(l')] = \delta_{l,l'}$, and similar expressions for \bar{q} , $\bar{\varphi}_o$ and $\bar{c}(l)$, $\bar{c}^\dagger(l)$. Returning to the vertex operators, which are our main interest in this appendix, we notice that, in operator formalism, it is necessary to normal-order them as follows:

$$V_\beta(z) = : e^{i\beta\varphi(z)} : = e^{-i\beta\varphi_o} e^{\beta q \log z} e^{i\beta \sum_{l>0} z^l c^\dagger(l)/\sqrt{l}} e^{i\beta \sum_{l>0} z^{-l} c(l)/\sqrt{l}}, \quad (\text{B16})$$

and a similar expression holds for the vertex operators of $\bar{\varphi}(\bar{z})$. This is needed in order to avoid divergences, which are related to the “charge self-energy” problem encountered above when using the functional integral approach. With these provisos, the probability distribution of the Laughlin state can be written as:

$$P_m(\mathbf{r}_1, \dots, \mathbf{r}_N) = \bar{\Phi}_m(\bar{z}_1, \dots, \bar{z}_N) \Phi_m(z_1, \dots, z_N), \quad (\text{B17})$$

where

$$\bar{\Phi}_m(\bar{z}_1, \dots, \bar{z}_N) = \langle \bar{V}_{-\sqrt{m}}(\bar{z}_1) \dots \bar{V}_{-\sqrt{m}}(\bar{z}_N) : e^{\int_{|z|<R} d^2z \bar{\varphi}(\bar{z}) \rho_0} \rangle, \quad (\text{B18})$$

$$\Phi_m(z_1, \dots, z_N) = \langle V_{+\sqrt{m}}(z_1) \dots V_{+\sqrt{m}}(z_N) : e^{\int_{|z|<R} d^2z \varphi(z) \rho_0} \rangle. \quad (\text{B19})$$

Therefore, the probability distribution for the Laughlin state splits into the product of two correlation functions of the gaussian theory. Let us now demonstrate that each of these equals either the Laughlin state or its anti-analytic version (i.e. its complex conjugate). To this end, it is useful to further investigate some of the properties of the vertex operators. For example, their two-point correlation function reads:

$$\langle V_\beta(z) V_{-\beta}(z') \rangle = (z - z')^{-\beta^2}, \quad (\text{B20})$$

as it can be shown from the identity $e^A e^B = e^C e^B e^A$ for any two operators with a c-number commutator $C = [A, B]$. The generalization to multi-point correlation functions can be obtained in a similar fashion:

$$\langle V_{\beta_1}(z_1) \dots V_{\beta_N}(z_N) \rangle = \prod_{i<j} (z_i - z_j)^{\beta_i \beta_j} \quad (\text{B21})$$

provided that $\sum_{i=1}^N \beta_i = 0$. Using this result, it can be shown that

$$\Phi_m(z_1, \dots, z_N) = e^{i w(z_1, \dots, z_N)} \prod_{i<j} (z_i - z_j)^m \prod_{i=1}^N e^{-|z_i|^2/2\ell^2}, \quad (\text{B22})$$

i.e. the Laughlin state. The phase factor $e^{i w(z_1, \dots, z_N)}$ cancels out after taking the product with the anti-analytic part $\bar{\rho}(\bar{z}_1, \dots)$, and we shall not consider it any further.

To end this discussion, let us make firmer the connection to the low-energy description of surface modes, which we have loosely established above. This can be achieved by a re-examination of the field operator found in Sect. III. There we showed that the boson field operator is related to the operator $e^{\pm i m \phi(\theta)}$, which can be shown to be proportional to a vertex operator. Indeed, if we normal order it properly, we obtain (α is a short distance cut-off):

$$e^{\pm i m \phi(\theta)} = \alpha^{m/2} e^{-i m \theta/2} : e^{\pm i m \phi(\theta)} :. \quad (\text{B23})$$

We next notice that by comparing the mode expansions, Eq (B15) and Eq. (21), one can identify $\phi(\theta) = \bar{\varphi}(\bar{z} = e^{-i\theta})/\sqrt{m}$. Thus we arrive at

$$\Psi(\theta) = A e^{+i m (N-1)\theta} \bar{V}_{+\sqrt{m}}(\bar{z} = e^{-i\theta}), \quad (\text{B24})$$

$$\Psi^\dagger(\theta) = A e^{i m N \theta} \bar{V}_{-\sqrt{m}}(\bar{z} = e^{-i\theta})., \quad (\text{B25})$$

from which one can readily show that the one-body density matrix at the boundary,

$$G(\theta - \theta') = \langle \Psi^\dagger(\theta) \Psi(\theta') \rangle = \text{const} \times e^{-i m l_0 (\theta - \theta')} \left[\sin \left(\frac{(\theta - \theta')}{2} \right) \right]^{-m}, \quad (\text{B26})$$

as follows from Eqs. (B24, B25), and (B20). Therefore, if we define the boson operator in the LLL as $\Psi_B^\dagger(\bar{z}) \equiv \bar{V}_{-\sqrt{m}}(\bar{z})$, the Laughlin wave function can be written in the very appealing way,

$$\bar{\Phi}_m(\bar{z}_1, \dots, \bar{z}_N) = \langle \Psi_B^\dagger(\bar{z}_1) \dots \Psi_B^\dagger(\bar{z}_N) : e^{\int_{|z|<R} d^2z \bar{\varphi}(\bar{z}) \rho_0} \rangle. \quad (\text{B27})$$

This is the main result of this appendix.

[1] A discussion of the role of broken Galilean and $U(1)$ Gauge invariance in classical and quantum fluids can be found in A. M. J. Schakel, *Boulevard of Broken Symmetries*, cond-mat/9805152. As explained by Schakel, another consequence of broken Galilean invariant is the existence of sound waves, which are the Goldstone modes.

- [2] Vorticity, $\omega = \nabla \times \mathbf{v}$, is strictly conserved in a classical fluid for isentropic (i.e. dissipationless) flow.
- [3] J. R. Abo-Shaeer *et al.*, Science **292**, 476 (2000).
- [4] In this work we shall assume that the trapping potential may be anisotropic, with $\omega_{||} \geq \omega_{\perp}$, where $\omega_{||}$ is the trap frequency along the rotation axis, Z, and ω_{\perp} the trap frequency perpendicular to Z.
- [5] N. R. Cooper, N. K. Wilkin, and J. M. F. Gunn, Phys. Rev. Lett. **87**, 120405 (2001).
- [6] N. Regnault and T. Jolicoeur, report cond-mat/0212477.
- [7] J. Sinova, C. B. Hanna, and A. H. MacDonald, Phys. Rev. Lett. **89**, 030403 (2002).
- [8] T. K. Gosh and G. Baskaran, cond-mat/0207484.
- [9] P. Rosenbusch *et al.*, Phys. Rev. Lett. **88**, 250403 (2002).
- [10] N. R. Cooper and N. K. Wilkin, Phys. Rev. B **60**, R16279 (1999).
- [11] N. K. Wilkin and J. M. F. Gunn, Phys. Rev. Lett. **84**, 6 (2000).
- [12] P. Engels, I. Coddington, P. C. Haljan, and E. A. Cornell, Phys. Rev. Lett. **89**, 100403 (2002).
- [13] T. L. Ho, Phys. Rev. Lett. **87**, 060403 (2001).
- [14] R. B. Laughlin, Phys. Rev. Lett. **50**, 1395 (1983).
- [15] D. Yoshioka, *The Quantum Hall Effect*, Springer-Verlag (Berlin, 2002).
- [16] A. Yu. Kitaev, quant-ph/9707021.
- [17] B. Paredes, P. Fedichev, J. I. Cirac, and P. Zoller, Phys. Rev. Lett. **87**, 010402 (2001).
- [18] B. Paredes, P. Zoller, and J. I. Cirac, Phys. Rev. A **66**, 033609 (2002).
- [19] X.-G. Wen, Int. J. of Mod. Phys. **6**, 1711 (1992).
- [20] X.-G. Wen, Adv. in Phys. **44**, 405 (1995).
- [21] T. L. Ho and E. Mueller, Phys. Rev. Lett. **89**, 050401 (2002).
- [22] D. Jaksch, talk presented at the workshop on Ultra-cold Diluted Gases, held in Benasque (Spain), July 2002.
- [23] J. W. Reijnders *et al.*, Phys. Rev. Lett. **89**, 120401 (2002).
- [24] F. D. M. Haldane, Bull. Am. Phys. Soc. **35**, 254 (1990); unpublished.
- [25] F. D. M. Haldane, Phys. Rev. Lett. **67**, 937 (1991).
- [26] M. Stone, H. W. Wyld, and R. L. Schult, Phys. Rev. B **45**, 14156 (1992).
- [27] N. Read and E. H. Rezayi, Phys. Rev. B **59**, 8084 (1999).
- [28] J. K. Jain and T. Kawamura, Europhysics Letters **29**, 321 (1995).
- [29] Y.-S. Wu, Phys. Rev. Lett. **73**, 922 (1992).
- [30] S. Viefers, T. H. Hansson, and S. M. Reimann, Phys. Rev. A **62** 053604 (2000).
- [31] R. A. J. van Elburg and K. Schoutens, Phys. Rev. B **58** 15704 (1998).
- [32] D. M. Stamper-Kurn *et al.*, Phys. Rev. Lett. **83**, 2876 (1999).
- [33] D.-H. Lee and X.-G. Wen, Phys. Rev. Lett. **66**, 347 (1991).
- [34] S. S. Mandal and J. K. Jain, to appear in Phys. Rev. Lett., cond-mat/0207615.
- [35] A. H. MacDonald and S. M. Girvin, Phys. Rev. B **39**, 6295 (1988).
- [36] A. Cappelli, C. Méndez, G. R. Zemba, Phys. Rev. B **58**, 16291 (1998).
- [37] X. G. Wen, Mod. Phys. Lett. B, **5**, 39 (1991).
- [38] F. D. M. Haldane, Phys. Rev. Lett. **51**, 605 (1983).
- [39] D. Forster, *Hydrodynamics fluctuations, Broken symmetry, and correlation functions*, (W. A. Benjamin, Reading, MA, 1975).
- [40] D. V. Petrov, M. Holzmann, and G.V. Shlyapnikov, Phys. Rev. Lett. **84**, 2551 (2000).
- [41] J. M. Luttinger, Phys. Rev. **119**, 1153 (1960).
- [42] S. Mitra and A. H. MacDonald, Phys. Rev. B **48**, 2005 (1993).
- [43] Yu. Kagan, B.V. Svistunov, and G.V. Shlyapnikov, JETP Lett. **48**, 56 (1988).
- [44] M. Milovanović and N. Read, Phys. Rev. B **53**, 13559 (1996).
- [45] M. Huerta, *private communication*.
- [46] F. D. M. Haldane, *Luttinger's Theorem and Bosonization of the Fermi Surface in Perspectives in Many-Body Physics* (Proceedings of the International School "Enrico Fermi", Varenna on Lake Como, 1992). Edited by A. Broglia and J. R. Schrieffer, (North Holland, Amsterdam, 1994), pag. 5-29.
- [47] B. I. Halperin, Helv. Phys. Acta **56**, 75 (1983).
- [48] C. J. Myatt *et al.*, Phys. Rev. Lett. **78**, 586 (1997).
- [49] C. J. Pethick and H. Smith, *Bose-Einstein Condensation in Dilute Gases* (Cambridge University Press, Cambridge, 2002).
- [50] W. Ketterle, *Spinor Condensates and Light Scattering from Bose-Einstein Condensates*, Proceedings of Les Houches 1999 Summer School, Session LXXII, cond-mat/0005001
- [51] S. K. Yip, Phys. Rev. B **43**, 1707 (1991).
- [52] E. Lipparini *et al.*, Phys. Rev. **56**, 12375 (1997).
- [53] G. Moore and N. Read, Nucl. Phys. B **360**, 362 (1991).
- [54] A. M. Tsvelik, *Quantum Field Theory in Condensed Matter* (Cambridge University Press, Cambridge, 1995).
- [55] In what follows, we shall also denote by S the hyperfine spin F .